NTIA Report 98-344

Analysis and Calculations of the Ground Plane Inductance Associated with a Printed Circuit Board

Christopher L. Holloway
Edward F. Kuester

U.S. DEPARTMENT OF COMMERCE
William M. Daley, Secretary

Larry Irving, Assistant Secretary
for Communications and Information

November 1997

CONTENTS

Page

FIGURES

Page

ANALYSIS AND CALCULATIONS OF THE GROUND PLANE INDUCTANCE ASSOCIATED WITH A PRINTED CIRCUIT BOARD

Christopher L. Holloway[1]
Edward F. Kuester[2]

A knowledge of the net inductance of the ground plane can aid in the analysis and investigation of printed circuit board emissions. In this report, we present a method, based on the concept of partial inductance, to determine the net inductance of the ground plane associated with a microstrip line. This method is based on a previously derived expression for the current density on the ground plane. We show calculations for the net, self-partial, and mutual-partial inductance of the ground plane for various trace geometries of practical interest. We also illustrate how the classical transmission line inductance of a microstrip line can be obtained from the concept of partial inductance. Comparisons to different experimental results are also given.

Key words: net inductance; partial inductance; ground plane inductance; common-mode emissions; microstrip line inductance; printed circuit board emission

1. INTRODUCTION

Printed circuit boards (PCBs) are the focus of many design efforts to comply with domestic and international electromagnetic compatibility (EMC) requirements for digital devices [1]. These boards are the root of most emission and immunity problems; hence, properly designed PCBs can offer a cost-effective approach to achieving EMC compliance [2] and [3].

PCBs produce two types of radiated emissions: differential-mode and common-mode [3]-[6]. Differential-mode or loop emissions are the result of currents that flow on a signal trace between integrated circuits (ICs), and return via a trace, grid, or plane. Fortunately, the signal-trace current produces fields that tend to cancel the fields from the ground-return current [4], [7], and [8]. Hence, typical signal currents must flow through relatively large PCB loops to produce emissions that exceed the regulatory limits. In these cases, the emissions can be reduced by simply placing the signal trace closer to the ground return and/or reducing the distance between the source and load ICs.

[1] The author is with the Institute for Telecommunications Sciences, National Telecommunications and Information Administration, U.S. Department of Commerce, Boulder Laboratories, Boulder, CO, 80303

[2] The author is with the Department of Electrical and Computer Engineering, University of Colorado, Boulder, CO, 80309-0424

Common-mode emissions are predominantly caused by unbalanced interconnections between digital circuits. Even a slight difference in the geometry of the signal and ground-return conductors on a PCB or in an IC package can cause common-mode currents to flow. These currents are problematic because they flow in a common direction and produce fields that tend to add to one another [4], [7], and [8]. Hence, common-mode currents can be several orders of magnitude less than differential-mode currents, but produce the same level of radiated emissions. Attaching cables to the PCB simply increases the length of the antenna and reduces the resonant frequency at which the maximum radiated emissions occur.

An unbalanced circuit on a PCB constructed with signal and ground-return trace pairs will radiate as an asymmetric folded-dipole [9]. Since the rectangular geometry of IC packages is inherently unbalanced, it is virtually impossible to construct balanced circuits on a PCB using ground-return traces. Even simple circuits will produce fields that exceed the regulatory limits [4], [8], and [9]. One solution to this difficult problem is to place a relatively large conducting plane beneath the PCB. The currents induced on this image plane will produce fields that tend to cancel the fields produced by the common-mode currents on the PCB, which causes a dramatic reduction in the total radiated emissions [9]-[11].

Image currents can also lower emissions from PCBs constructed with a ground-return plane or an equivalent ground-return grid [2] and [12]-[15]. Indeed, common-mode currents cannot flow on a PCB with an infinite ground-return plane because the signal conductor and its ground-plane image are perfectly balanced. However, the finite ground-return plane on an actual PCB produces an imperfect image that causes the ground-return plane itself to radiate as a dipole antenna [16] and [17]. In this case, the ground-noise voltage produced when signal currents encounter the impedance of the ground-return plane (referred to simply as a ground plane throughout the rest of this report) is the source driving the dipole antenna [3]. Once again, attaching cables to the PCB simply increases the dipole length. Even PCBs with a solid ground-return plane without attached cables can produce radiated emissions that exceed the Federal Communication Commission (FCC) Class-B limit [18].

The analysis of the actual problem of an imperfect image ground plane with unbalanced currents and attached cables (Figure 1) is a difficult one. However, by investigating the ground voltage-drop of a signal trace over a perfectly conducting infinitely large ground plane (microstrip line; Figure 2), one can determine how to reduce the ground voltage-drop (which is the source driving the emissions) of the actual problem. Using Faraday's law, it can be shown that a trace above a ground plane produces a voltage-drop on the ground plane directly under the trace. Furthermore, Faraday's law shows that this voltage-drop is related to the so-called net inductance [2] of the ground plane by the following [2] and [19]-[22]:

$$V_{gr} = L_{gr} \frac{\partial I}{\partial t}, \tag{1}$$

where L_{gr} is the net inductance of the ground plane. From this equation, it is evident that an understanding of the net inductance is imperative to the effective reduction of the ground plane voltage-drop and the resulting common-mode emissions in the actual problem.

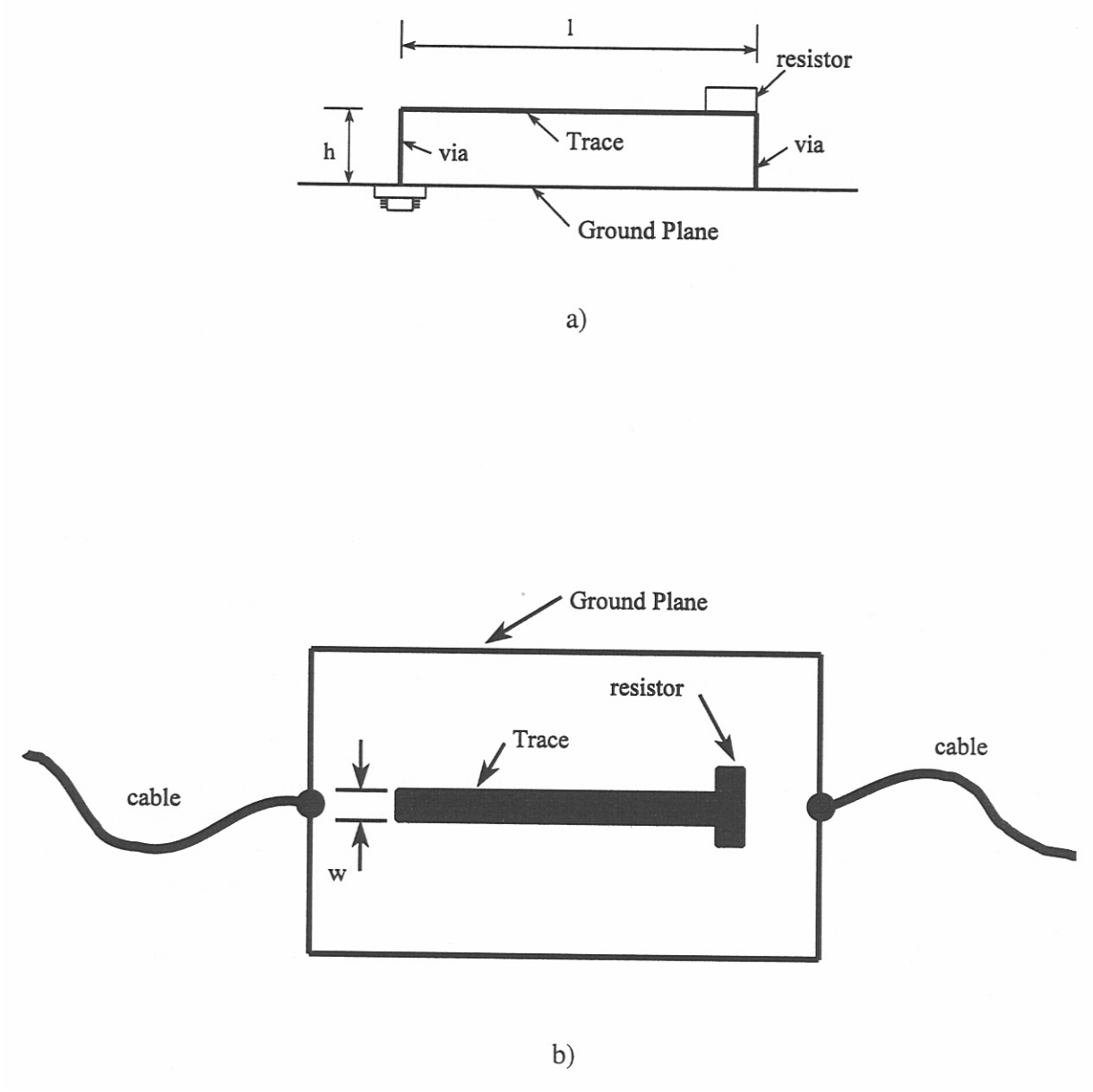

Figure 1. a) Side and b) top view of a trace over a ground plane with attached cables.

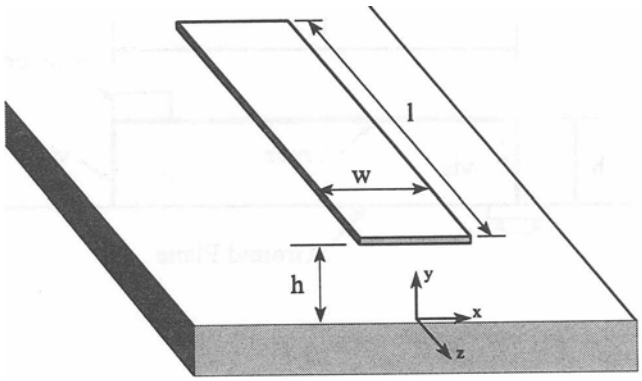

Figure 2. Trace over a ground plane: microstrip line.

Attempts have been made to calculate the ground plane net inductance with little success. Most recently Leferink and van Doorn [23] introduced a closed form expression for the net inductance for the ground plane. The expression assumes that the current on the ground plane is uniformly distributed over the entire ground, which is not the case (see [24] and [25]). This expression indicates that if the width of the ground plane becomes very large, then the ground plane inductance approaches zero.

In this report, we present a technique for calculating the net inductance of the ground plane, using the actual current distribution on the ground plane. This report is organized as follows: Section 2 illustrates the concepts of partial inductance and shows how they are related to the voltage drop across the ground plane. In Section 3, we introduce a procedure to calculate the net inductance of both the ground plane and the trace based on the knowledge of the current distribution on the ground plane. Section 4 discusses the numerical implementation of the results given in Section 3. In Section 5 we show results for the net, self-partial, and mutual-partial inductance of the ground plane and trace for various circuit geometries of practical interest. Finally, we discuss effects of current constriction due to vias on the net inductance of the ground plane.

2. CONCEPTS OF PARTIAL INDUCTANCE

Much has been written on the subject of partial inductance, for details see [2], [9], and [19]-[22]. The origin for this material dates back to the turn of the century with the work of Wien [26], Rosa [27], and Rosa and Grover [28]. This section provides a brief overview of the subject and its application to transmission lines. Assuming there is a rectangular loop of wire carrying current (Figure 3), the inductance of this loop is given by the classical

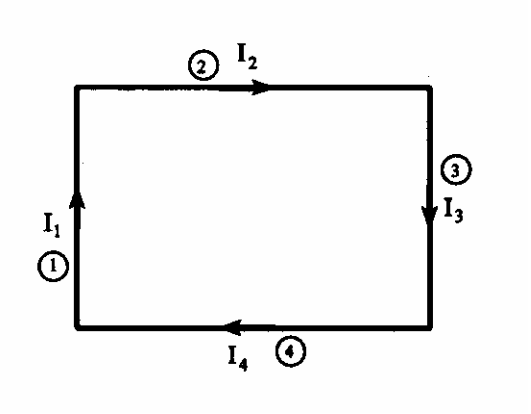

Figure 3. Current loop.

expression:

$$L = \frac{\int_s \overline{B} \cdot d\overline{s}}{I}, \tag{2}$$

where $\overline{B}$ is the magnetic field flowing through the loop cross-section and I is the total current flowing through the loop.

Recall that the magnetic field $\overline{B}$ can be represented in terms of a magnetic potential $\overline{A}$ by the following:

$$\overline{B} = \nabla \times \overline{A}. \tag{3}$$

With this expression and Stokes' theorem, the inductance of the loop can be written as:

$$L = \frac{\oint_c \overline{A} \cdot d\overline{l}}{I}, \tag{4}$$

where c is the contour of the loop.

This integral can be broken into the following four segments:

$$\begin{aligned} L &= \frac{\int_{c1} \overline{A} \cdot d\overline{l}_1}{I} + \frac{\int_{c2} \overline{A} \cdot d\overline{l}_2}{I} + \frac{\int_{c3} \overline{A} \cdot d\overline{l}_3}{I} + \frac{\int_{c4} \overline{A} \cdot d\overline{l}_4}{I} \\ &= L_1 + L_2 + L_3 + L_4, \end{aligned} \tag{5}$$

where c_i are the contours of each segment. Each L_i represents the contribution of each segment to the total inductance, and is called the net inductance of each segment of line [2]:

$$L_i = \frac{\int_{c_i} \overline{A} \cdot d\overline{l}_i}{I}. \tag{6}$$

The net inductance of each segment can be expressed as the sum of self- and mutual-partial inductances for the segment, and can be written as:

$$L_i = \sum_{j=1}^{N} \pm L_{p_{ij}}, \tag{7}$$

where N is the total number of segments. If $i = j$, then $L_{p_{ij}}$ corresponds to the self-partial inductance. If $i \neq j$, then $L_{p_{ij}}$ corresponds to the mutual-partial inductance. The sign (±) is related to the relative orientation of the current in segment j to the current in segment i, and is determined by the sign of the dot product between directed current elements. The concept of mutual-partial inductance is equivalent to the mutual inductance associated with adjacent circuits that couple to one another [29] (i.e., the mutual-partial inductance is associated with coupling of the different segments).

The partial inductance $L_{p_{ij}}$ is defined as the ratio of the magnetic flux penetrating the surface between segment i and infinity and current I_j that produces that flux. $L_{p_{ij}}$ can be written as:

$$L_{p_{ij}} = \frac{\int_{c_i} \overline{A}_{ij} \cdot d\bar{l}_i}{I_j}. \tag{8}$$

The classical inductance of the loop can be written in terms of the net inductance. Using equations (5) and (7),

$$L = \sum_{i=1}^{N} L_i = \sum_{i=1}^{N} \sum_{j=1}^{N} \pm L_{p_{ij}}. \tag{9}$$

The voltage drop across any segment of the loop can be expressed in terms of the net inductance of that segment. For example, the voltage across segment 1 can be expressed as:

$$V_1 = L_1 \frac{\partial I_1}{\partial t} \tag{10}$$

where $L_1 = L_{p_{11}} - L_{p_{13}}$ and is the net inductance of segment 1. Equation (6) indicates that a mutual-partial inductance exists only between segments that are not perpendicular to each other. Thus, there is no $L_{p_{12}}$ or $L_{p_{14}}$ term in the expression for the net inductance of segment 1.

2.1 Partial Inductance of Wires

The net and partial inductance of parallel wires has been obtained in the past and can be found in [2], [19]-[20] and [27]. The self- and mutual-partial inductances are given by the following:

$$L_{p_{ii}} = \frac{\mu}{2\pi} l \left\{ \ln \left[\frac{l}{r} + \sqrt{\left(\frac{l}{r}\right)^2 + 1} \right] + \frac{r}{l} - \sqrt{\left(\frac{r}{l}\right)^2 + 1} \right\} \tag{11}$$

and

$$L_{p_{ij}} = \frac{\mu}{2\pi} l \left\{ \ln \left[\frac{l}{d} + \sqrt{\left(\frac{l}{d}\right)^2 + 1} \right] + \frac{d}{l} - \sqrt{\left(\frac{d}{l}\right)^2 + 1} \right\}, \tag{12}$$

where d is the separation of the two wires, r is the radius of the wires, and l is the length of the wires. When the length l of the wires is large compared to the radius r and the separation d, equations (12) and (11) can be approximated by:

$$L_{p_{ii}} \approx \frac{\mu}{2\pi} l \left[\ln\left(\frac{2l}{r}\right) - 1 \right] \text{ for } \frac{r}{l} << 1 \tag{13}$$

and

$$L_{p_{ij}} \approx \frac{\mu}{2\pi} l \left[\ln\left(\frac{2l}{d}\right) - 1 + \frac{d}{2l} \right] \text{ for } \frac{r}{l} << 1 \text{ and } \frac{d}{l} << 1 . \tag{14}$$

For parallel conductors of rectangular cross-section, the mutual-partial inductance is given by equation (14) and the self-partial inductance is given by:

$$L_{p_{ii}} \approx \frac{\mu}{2\pi} l \left[\ln\left(\frac{8l}{w}\right) - 1 \right] \text{ for } \frac{w}{l} << 1 \text{ and } \frac{w}{l} << 1 , \tag{15}$$

where w and t are width and thickness of the trace, respectively. See [19] and [22] for expressions of the net and partial inductance for wires of different orientations.

3. NET INDUCTANCE OF THE GROUND PLANE AND TRACE

The problem of interest in this report is that of a trace suspended over a ground plane (see Figure 2). The equation given in Section 2 for the partial inductance (see equation (8)) is for conductors with a current filament. However, the current density in the ground plane is not a constant, nor is it concentrated under the trace. The current spreads out from under the trace, and in previous work ([24] and [25]) the following expression was derived for the current density on the ground plane:

$$J_{gr}(x) = \frac{I}{w\pi} \left[\tan^{-1}\left(\frac{w-2x}{2h}\right) + \tan^{-1}\left(\frac{w+2x}{2h}\right) \right], \tag{16}$$

where W is the width of the trace and h is the height of the trace above the ground. Thus, the procedure given in Section 2 for calculating the net, self-partial, and mutual-partial inductance must be modified to account for this type of current distribution.

The basic concept of inductance must be used to obtain an expression of the net inductance of the ground plane and the trace. The inductance of this microstrip geometry of length l is given by:

$$L = \frac{2U}{I^2}, \tag{17}$$

where U is the stored energy within the volume bound by the ground plane and the trace, and is given by:

$$U = \frac{1}{2} \int_v \overline{B} \cdot \overline{H} \, dv . \tag{18}$$

The inductance can then be given by:

$$L = \frac{1}{I^2}\int_v \overline{B}\cdot\overline{H}\ dv\,. \tag{19}$$

When $\overline{B}$ is replaced with ∇ x $\overline{A}$, L can be written as:

$$L = \frac{1}{I^2}\int_v \nabla\times\overline{A}\cdot\overline{H}\ dv\,. \tag{20}$$

The integrand can be rewritten with the aid of a vector identity as:

$$\overline{H}\cdot\left(\nabla\times\overline{A}\right) = \nabla\cdot\left(\overline{A}\times\overline{H}\right) + \overline{A}\cdot\left(\nabla\times\overline{H}\right). \tag{21}$$

The $\overline{H}$ field in this expression is related to the volume current density by Maxwell's equations:

$$\nabla\times\overline{H} = \bar{J}_v\,. \tag{22}$$

For this problem, the volume current density J_v is zero. Thus, equation (20) reduces to the following:

$$L = \frac{1}{I^2}\int_v \nabla\cdot\left(\overline{A}\times\overline{H}\right) dv\,. \tag{23}$$

With the divergence theorem, this integral becomes:

$$L = \frac{1}{I^2}\int_s \left(\overline{A}\times\overline{H}\right)\cdot\bar{a}_n ds\,, \tag{24}$$

where s consists of three parts (Figure 4). The first is the surface of the ground plane s_{gr}, the second is the surface of the top and bottom portions of the trace s_{tr}^{top} and s_{tr}^{bottom}, and the third is the surface surrounding the ground plane and trace s_1. The fields decay to zero as the surface s_1 is moved to infinity. Therefore, the surface integral in equation (24) reduces to an integration only over s_{gr}, s_{tr}^{top}, and s_{tr}^{bottom}.

The integrand of this integral can be rewritten as:

$$\bar{a}_n\cdot\left(\overline{A}\times\overline{H}\right) = \overline{A}\cdot\left(\overline{H}\times\bar{a}_n\right). \tag{25}$$

When equation (25) is substituted into equation (24), the following is obtained:

$$\begin{aligned} L \;=\; & \tfrac{1}{I^2}\int_{s_{gr}} \bar{A}\cdot(\bar{H}\times\bar{a}_n)ds_{gr} + \tfrac{1}{I^2}\int_{s_{tr}^{top}} \bar{A}\cdot(\bar{H}\times\bar{a}_n)ds_{tr}^{top} \\ & + \tfrac{1}{I^2}\int_{s_{tr}^{bottom}} \bar{A}\cdot(\bar{H}\times\bar{a}_n)ds_{tr}^{bottom} \end{aligned} \tag{26}$$

The boundary conditions on Maxwell's equations allow the $\overline{H}$ to be related to the current density on the ground plane J_{gr} and on the trace J_{tr}:

$$\begin{aligned} \bar{a}_n\times\bar{H}_{gr} &= -\bar{a}_z J_{gr} \\ \bar{a}_n\times\bar{H}_{tr}^{top,bottom} &= \bar{a}_z J_{tr}^{top,bottom}\,. \end{aligned} \tag{27}$$

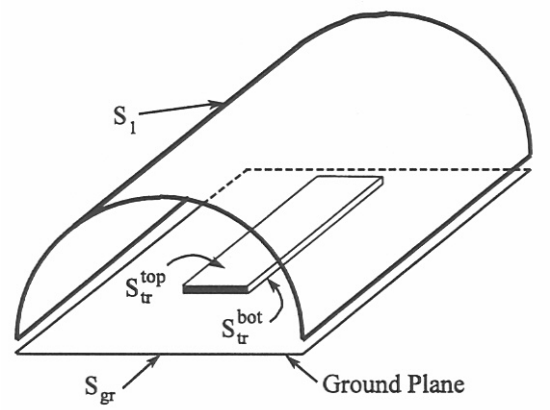

Figure 4. Definition of surfaces needed in the evaluation of the integral for calculating the inductance.

The minus sign accounts for the current on the ground plane flowing in the opposite direction (the minus z direction) from that of the current on the trace.

We showed in [30] that for most practical microstrip geometries, the current densities on the top and bottom surface of the trace are equivalent and are approximated by:

$$J_{tr}^{top} \approx J_{tr}^{bottom} \approx \frac{J_{tr}}{2}, \tag{28}$$

where J_{tr} is the total current density on the strip. Thus the inductance of the microstrip line reduces to the following:

$$\begin{aligned} L \;=\; & +\tfrac{1}{I^2}\int_{x=-w/2}^{w/2}\int_{z=0}^{l} J_{tr}(x)\,A_z(x,z)\,dx\,dz \\ & -\tfrac{1}{I^2}\int_{x=-\infty}^{\infty}\int_{z=0}^{l} J_{gr}(x)\,A_z(x,z)\,dx\,dz\;, \end{aligned} \tag{29}$$

where J_{gr} is the current density on the ground plane as given in equation (16), J_{tr} is the total current density on the trace (see section 3.2), and A_z is the magnetic potential produced by both the ground plane and trace current densities.

Equation (29) can be broken into two parts:

$$L = L_{gr} + L_{tr}, \tag{30}$$

where L_{gr} is the net inductance of the ground plane, and

$$L_{gr} = -\frac{1}{I^2}\int_{x=-\infty}^{\infty}\int_{z=0}^{l} J_{gr}(x)A_z(x,z,y=0)\,dx\,dz, \tag{31}$$

where the minus sign indicates that the current on the ground plane flows in the minus z direction. L_{tr} is the net inductance of the trace:

$$L_{tr} = \frac{1}{I^2}\int_{x=-w/2}^{w/2}\int_{z=0}^{l} J_{tr}(x)A_z(x,z,y=h)\,dx\,dz \tag{32}$$

where $y = 0$ corresponds to the location of the ground plane on the y axis and $y = h$ corresponds to the location of the trace on the y axis.

To obtain an expression for these net inductances, an expression for the magnetic vector potential A_z is needed. A_z has contributions from the currents on both the ground plane and the trace, and is determined from a standard quasi-static Green's function approach:

$$A_z(x,z,y) = A_z^{gr}(x,z,y) + A_z^{tr}(x,z,y)\ , \tag{33}$$

where $A_z^{gr}(x,z,y)$ is the portion of the total potential produced by the currents flowing on the ground:

$$A_z^{gr}(x,z,y) = -\mu_0 \int_{x'=-\infty}^{\infty} \int_{z'=0}^{l} J_{gr}(x')\, G(x,x',z,z',y,y'=0)\, dx'\, dz' \tag{34}$$

and $A_z^{tr}(x,z,y)$ is the portion of the total potential produced by the current flowing on the trace:

$$A_z^{tr}(x,z,y) = \mu_0 \int_{x'=-w/2}^{w/2} \int_{z'=0}^{l} J_{tr}(x')\, G(x,x',z,z',y,y'=h)\, dx'\, dz'\ , \tag{35}$$

where G is the free space Green's function given by:

$$G = \frac{1}{4\pi} \frac{1}{\sqrt{(x-x')^2 + (z-z')^2 + (y-y')^2}}\ . \tag{36}$$

With equations (31), (34), and (35), the net inductance of the ground plane reduces to:

$$\begin{aligned} L_{gr} \;=\; & \tfrac{\mu}{4\pi I^2} \int_{x=-\infty}^{\infty} \int_{z=0}^{l} J_{gr}(x) \\ & \left[\int_{x'=-\infty}^{\infty} \int_{z'=0}^{l} J_{gr}(x') G(x,x',z,z',y=0,y'=0)\, dx' dz' \right]\ dx\, dz \\ & -\tfrac{\mu}{4\pi I^2} \int_{x=-\infty}^{\infty} \int_{z=0}^{l} J_{gr}(x) \\ & \left[\int_{x'=-w/2}^{w/2} \int_{z'=0}^{l} J_{tr}(x') G(x,x',z,z',y=0,y'=h)\, dx' dz' \right]\ dx\, dz \end{aligned} \tag{37}$$

and with equations (32), (34), and (35), the net inductance of the trace reduces to

$$\begin{aligned} L_{tr} \;=\; & \tfrac{\mu}{4\pi I^2} \int_{x=-w/2}^{w/2} \int_{z=0}^{l} J_{tr}(x) \\ & \left[\int_{x'=-w/2}^{w/2} \int_{z'=0}^{l} J_{tr}(x') G(x,x',z,z',y=h,y'=h)\, dx' dz' \right]\ dx\, dz \\ & -\tfrac{\mu}{4\pi I^2} \int_{x=-w/2}^{w/2} \int_{z=0}^{l} J_{tr}(x) \\ & \left[\int_{x'=-\infty}^{\infty} \int_{z'=0}^{l} J_{gr}(x') G(x,x',z,z',y=h,y'=0)\, dx' dz' \right]\ dx\, dz \end{aligned} \tag{38}$$

3.1 Self-Partial Inductance of the Ground Plane

The self-partial inductance of the ground plane is defined as the inductance of the ground caused by the magnetic potential produced solely by the current flowing on the ground plane.

Thus, from equation (37) the self-partial inductance of the ground plane can be expressed as:

$$LS_{gr} = \frac{\mu_0}{4\pi I^2}\int_{x=-\infty}^{\infty} J_{gr}(x)\left[\int_{x'=-\infty}^{\infty} J_{gr}(x')K(x,x')\,dx'\right]dx\,, \tag{39}$$

where the kernel $K(x, x')$ contains the integrals over z and z′, and is given by:

$$K(x,x') = \int_{z=0}^{l}\left[\int_{z'=0}^{l}\frac{dz'}{\sqrt{(x-x')^2+(z-z')^2}}\right]dz\,. \tag{40}$$

This double integral is fairly simple and can be evaluated explicitly. Leaving out the details, it can be shown that once the z and z' integrals are evaluated, the kernel $K(x, x')$ reduces to the following:

$$K(x,x') = K_1(x,x') + K_2(x,x'), \tag{41}$$

where $K_1(x, x')$ is the nonsingular part, and is expressed as:

$$K_1(x,x') = 2|x-x'| - 2\sqrt{(x-x')^2+l^2} + 2l\ln\left(l+\sqrt{(x-x')^2+l^2}\right) \tag{42}$$

and $K_2(x, x')$ is the singular part, and is expressed as:

$$K_2(x,x') = -2l\ln(|x-x'|)\,. \tag{43}$$

Therefore, the self-partial inductance of the ground is given by:

$$\begin{aligned} LS_{gr} \;=\; & \tfrac{\mu_o}{4\pi I^2}\int_{x=-\infty}^{\infty} J_{gr}(x)\left[\int_{x'=-\infty}^{\infty} J_{gr}(x')K_1(x,x')\,dx'\right]dx \\ & +\tfrac{\mu_o}{4\pi I^2}\int_{x=-\infty}^{\infty} J_{gr}(x)\left[\int_{x'=-\infty}^{\infty} J_{gr}(x')K_2(x,x')\,dx'\right]dx \end{aligned}\,. \tag{44}$$

Unfortunately, the two integrals in this expression cannot be evaluated in closed form and must be determined by numerical means. In Section 4, the numerical integration of these two integrals and the integrals evaluated in the next two sections are discussed.

3.2 Self-Partial Inductance of the Trace

The self-partial inductance of the trace is defined as the inductance of the trace caused by the magnetic potential produced solely by the current flowing on the trace. To calculate this quantity, two different expressions for the current density on the trace are used. For a $w/h \geq 0.5$, the current density on the trace is approximated by a constant distribution:

$$J_{tr} = \frac{I}{w} \tag{45}$$

and for $w/h < 0.5$, the current density is approximated by the Maxwell distribution:

$$J_{tr} = \frac{I}{\pi\sqrt{\left(\frac{w}{2}\right)^2 - x^2}}\,. \tag{46}$$

For the constant distribution, the self-partial inductance of the trace can be expressed as:

$$LS_{tr} = \frac{\mu_0}{4\pi w^2} \int_{x'=-w/2}^{w/2} \int_{x=-w/2}^{w/2} K(x,x')\, dx\, dx' \tag{47}$$

and for the Maxwell distribution, the self-partial inductance becomes

$$LS_{tr} = \frac{\mu_0}{4\pi^3} \int_{x'=-w/2}^{w/2} \frac{1}{\sqrt{\left(\frac{w}{2}\right)^2 - (x')^2}} \int_{x=-w/2}^{w/2} \frac{1}{\sqrt{\left(\frac{w}{2}\right)^2 - (x)^2}} K(x,x')\, dx\, dx' , \tag{48}$$

where the kernel $K(x,x')$ is given in equation (41). Note that equation (48) has an added singularity caused by the Maxwell distribution. Once again, this integral cannot be evaluated in closed form, and must be determined numerically.

3.3 Mutual-Partial Inductance of the Ground Plane and Trace

The mutual-partial inductance of the ground plane is defined as the inductance of the ground caused by the magnetic potential produced solely by the current flowing on the trace. Using equation (37), the mutual-partial inductance of the ground can be obtained. Once again the z and z' integral can be evaluated explicitly. If the x and x' integrals are interchanged, the following is obtained:

$$LM_{gr} = \frac{\mu_0}{4\pi l^2} \int_{x'=-w/2}^{w/2} J_{tr}(x') \int_{x=-\infty}^{\infty} J_{gr}(x)\, K_m(x,x')\, dx\, dx' , \tag{49}$$

where J_{tr} is given by either equation (45) or (46). Note that the mutual-partial inductance is defined as a positive quantity. In this equation, J_{gr} is given by equation (16) and the kernel $K_m(x, x')$ is given by:

$$\begin{aligned} K_m(x,x') &= 2\sqrt{(x-x')^2+h^2} - 2\sqrt{(x-x')^2+h^2+l^2} \\ &\quad + 2l \ln\left[\frac{l+\sqrt{(x-x')^2+h^2+l^2}}{\sqrt{(x-x')^2+h^2}}\right] \end{aligned} . \tag{50}$$

Once again, this integral cannot be evaluated in closed form, and must be determined numerically.

The mutual-partial inductance of the trace is obtained by using equation (38). Since the free space Green's function in this expression is symmetric in x and x', it can be shown that the mutual-partial inductance of the trace is identical to the mutual-partial inductance of the ground plane $LM_{tr} = LM_{gr}$.

3.4 Net Inductance

With the self- and mutual-partial inductance obtained, the net inductance of the ground plane can be expressed as:

$$L_{gr} = LS_{gr} - LM_{gr} , \tag{51}$$

and the net inductance of the trace is given by

$$L_{tr} = LS_{tr} - LM_{tr} \ . \tag{52}$$

4. NUMERICAL EVALUATION OF THE INTEGRALS

The integrals needed for the self-partial inductance of the ground are evaluated first. From Section 3, the self-partial inductance can be expressed as:

$$LS_{gr} = L_1 + L_2 \, , \tag{53}$$

where L_1 corresponds to the part of the inductance that has a nonsingular kernel in its integral and L_2 corresponds to the part of the inductance that has a singular kernel in its integral. These two terms are given by:

$$\begin{aligned} L_1 &= \frac{\mu_0}{4\pi I^2} \int_{x=-\infty}^{\infty} J_{gr}(x) \left[\int_{x'=-\infty}^{\infty} J_{gr}(x') K_1(x, x') \, dx' \right] dx \\ L_2 &= \frac{\mu_0}{4\pi I^2} \int_{x=-\infty}^{\infty} J_{gr}(x) \left[\int_{x'=-\infty}^{\infty} J_{gr}(x') K_2(x, x') \, dx' \right] dx \end{aligned} \tag{54}$$

where $K_1(x, x')$ and $K_2(x, x')$ are the nonsingular and singular kernels, respectively, and are given in equations (42) and (43).

The L_1 integral is fairly well behaved, and the only difficulty is that the limits of this double integral extend to infinity. The integral over x' (the inner integral) is evaluated with a 10-point quadrature rule (see [31]). The integration to $\pm\infty$ can be difficult to handle, but taking advantage of how the current on the ground is distributed can aid in evaluating these integrals. We showed in [24] that the amount of current that spreads out from under the trace is a function of the trace height h. For large h, the current spreads out far from the edge of the trace, and for small h the current is concentrated under the trace. To account for the rapid change in the ground plane current density in the vicinity of $x = w/2$, the integral is subdivided into fine cells around $x = w/2$. We also showed in [24] that at a location of about 100 w from the edge of the trace, the current is very small. The contribution of this small amount of current to the total integral in equations (44) and (49) is negligible. For assurance, these integrals are extended to $\pm(100000\ w)$. Therefore, the domain of the x' integral is divided into the following subdomains:

$$\begin{aligned} \int_0^{\infty} dx' \simeq & \int_o^{w/16} dx' + \int_{w/16}^{w/8} dx' + \int_{w/8}^{3w/16} dx' + \int_{3w/16}^{w/4} dx' + \int_{w/4}^{3w/8} dx' + \int_{3w/8}^{0.44w} dx' \\ & + \int_{0.44w}^{w/2-w/100} dx' + \int_{w/2-w/100}^{w/2-w/1000} dx' + \int_{w/2-w/1000}^{w/2} dx' + \int_{w/2}^{w/2+w/1000} dx' \\ & + \int_{w/2+w/1000}^{w/2+w/100} dx' + \int_{w/2+w/100}^{0.55w} dx' + \int_{0.55w}^{0.75w} dx' + \int_{0.75w}^{w} dx' + \int_{w}^{2w} dx' \\ & + \int_{2w}^{5w} dx' + \int_{5w}^{10w} dx' + \int_{10w}^{25w} dx' + \int_{25w}^{50w} dx' + \int_{50w}^{100w} dx' + \int_{100w}^{500w} dx' \\ & + \int_{500w}^{1000w} dx' + \int_{1000w}^{5000w} dx' + \int_{5000w}^{10000w} dx' + \int_{10000w}^{100000w} dx' \end{aligned} \ . \tag{55}$$

Similar expressions exist for the negative portion of the integral. Over each of these sub domains, the integral is approximated by the following 10-point Guassian quadrature formula:

$$\int_a^b f(x)dx \approx \sum_{i=1}^{N} A_i f(x_i), \tag{56}$$

where the weights A_i and abscissae x_i for a general purpose 10-point quadrature rule are given by Harris and Evans [31], and are listed in the Appendix. The details of the implementation of this technique can be found in [32].

The domain of the x integral (the outer integral) is divided into the same subdomains as in equation (55). Over each of these subregions, the integral is also approximated by a 10-point quadrature formula.

The L_2 integral poses an added difficulty, in that its kernel is singular and must be treated carefully. Harris and Evans [31] introduced an efficient general purpose 10-point quadrature formula for integrals with end point singular behavior. The weights A_i and abscissae x_i for this approach are given in [31], and are listed in the Appendix. As before, the inner and outer integrals (the x and x' integrals) are subdivided into the sub domains given in equation (55). Once again, the outer and inner integrals are evaluated with the general purpose 10-point quadrature rule. In order to take advantage of the efficient general purpose quadrature formula for endpoint singularities given in [31], the singular behavior of the kernel must be at the end point of the integrals given in equation (55). Therefore, a change of variable is needed for the inner integral to ensure that the singular behavior of the kernel in each subregion occurs at an end point. By using a change of variables where

$$t = x - x' \text{ and } dx' = -dt, \tag{57}$$

the integrals in equation (55) can be rewritten as:

$$\int_{x'=a}^{b} J_{gr}(x')\ln|x-x'|dx' = -\int_{t=x-a}^{t=x-b} J_{gr}(x-t)\ln(|t|)dt. \tag{58}$$

The numerical integration of the mutual-partial inductance [equation (49)] for the constant distribution is very similar to the evaluation of L_1. The main difference is that the outer limit of the integral is not extended to $\pm\infty$, but is evaluated to $\pm w/2$. The domain of the outer integral of equation (49) (the x' integral) is subdivided into the following subdomains:

$$\begin{aligned}\int_0^{\infty} dx' \simeq\ & \int_o^{w/16} dx' + \int_{w/16}^{w/8} dx' + \int_{w/8}^{3w/16} dx' + \int_{3w/16}^{w/4} dx' + \int_{w/4}^{3w/8} dx' + \int_{3w/8}^{0.44w} dx' \\ & + \int_{0.44w}^{w/2-w/100} dx' + \int_{w/2-w/100}^{w/2-w/1000} dx' + \int_{w/2-w/1000}^{w/2} dx'\end{aligned} \tag{59}$$

and the 10-point quadrature formula is used over each subdomain. The inner integral of equation (49) (the x integral) is subdivided as indicated in equation (55), and is evaluated with the general purpose 10-point quadrature procedure.

When the Maxwell current distribution is used in equations (48) and (49), the integrals have the following form:

$$\int_a^b \frac{1}{\sqrt{\left(\frac{w}{2}\right)^2 - x^2}} f(x)\, dx\,. \tag{60}$$

This integral needs to be modified to handle the singularity in J_{tr}. By using a change of variables where:

$$x = \frac{w}{2}\sin(\theta) \text{ and } dx = \frac{w}{2}\cos(\theta)\, d\theta\ , \tag{61}$$

the integral in equation (60) can be rewritten as:

$$\int_{\sin^{-1}(2a/w)}^{\sin^{-1}(2b/w)} f(\frac{w}{2}\sin(\theta))d\theta\,. \tag{62}$$

The evaluation of the self-partial inductance of the trace is similar to the determination of L_1 and L_2. The only difference is that for the trace, the limits of integration are $\pm w/2$.

5. CALCULATION OF THE NET AND PARTIAL INDUCTANCE

In this section, we present results of the net inductances $L_{gr,tr}$ (as well as the self-partial $LS_{gr,tr}$ and mutual-partial inductance $LM_{gr,tr}$) of both the ground plane and trace for various trace geometries of practical interest. Figures 5-7 show results for the self-partial inductance of the ground LS_{gr} as a function of the trace width w and the trace height h for trace lengths l of 2.54 cm (1 in), 15.24 cm (6 in), and 30.48 cm (12 in), respectively. Figures 8-10 show results of the mutual-partial inductance of the ground LM_{gr} as a function of the trace width w and the trace height h for trace lengths l of 2.54 cm, 15.24 cm, and 30.48 cm, respectively.

These figures indicate how the self- and mutual-partial inductances of the ground vary as a function of different geometries. The more important quantity needed to assess printed circuit board emissions is the net inductance $(LS_{gr} - LM_{gr})$ of the ground plane. This quantity can be obtained from equation (51). Figures 11-13 show results of the net inductance of the ground plane as a function of the trace width w and the trace height h for lengths l of 2.54 cm, 15.24 cm, and 30.48 cm, respectively. Figure 14 show results for the net inductance of the ground plane as a function 6f the trace height h, the trace width w, and the trace length l.

From these figures, it is apparent that the net inductance of the ground is less sensitive to the trace width w than it is to the trace height h. Two orders of magnitude change in the trace width results in only about a factor of 1.2-2.5 change in the net inductance of the ground. Whereas if the height of the trace is changed from 0.254 mm (10 mils) to 2.54 mm (100 mils), the net inductance changes by about a factor of 50. The smaller the height of the trace over the ground, the lower the net inductance, and more importantly, the lower the voltage-drop on the ground plane.

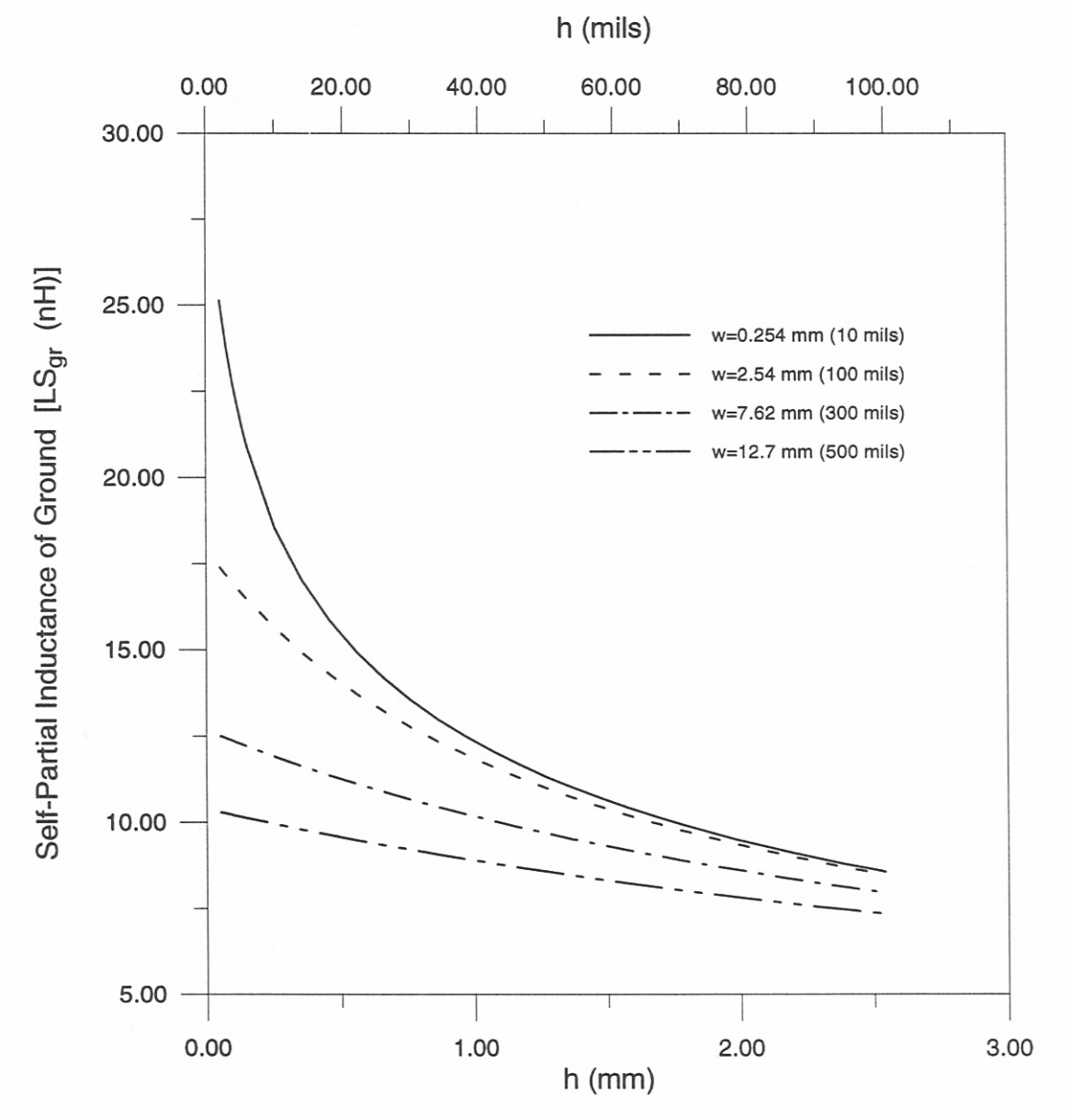

Figure 5. Self-partial inductance of the ground plane as a function of the trace width *w* and the height over the ground *h* for a trace length *l* of 2.54 cm (1 in).

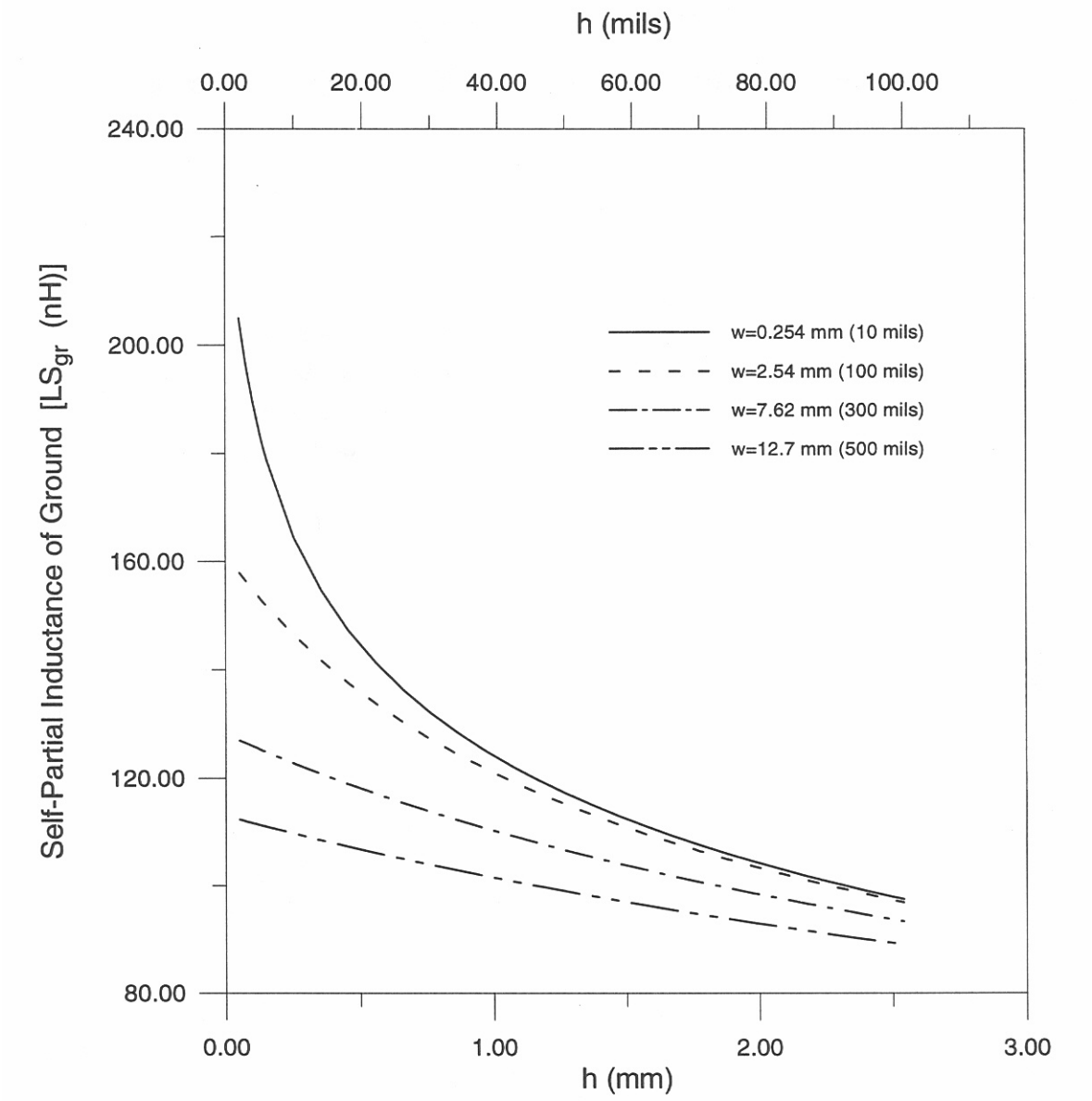

Figure 6. Self-partial inductance of the ground plane as a function of the trace width *w* and the height over the ground *h* for trace length *l* of 15.24 cm (6 in).

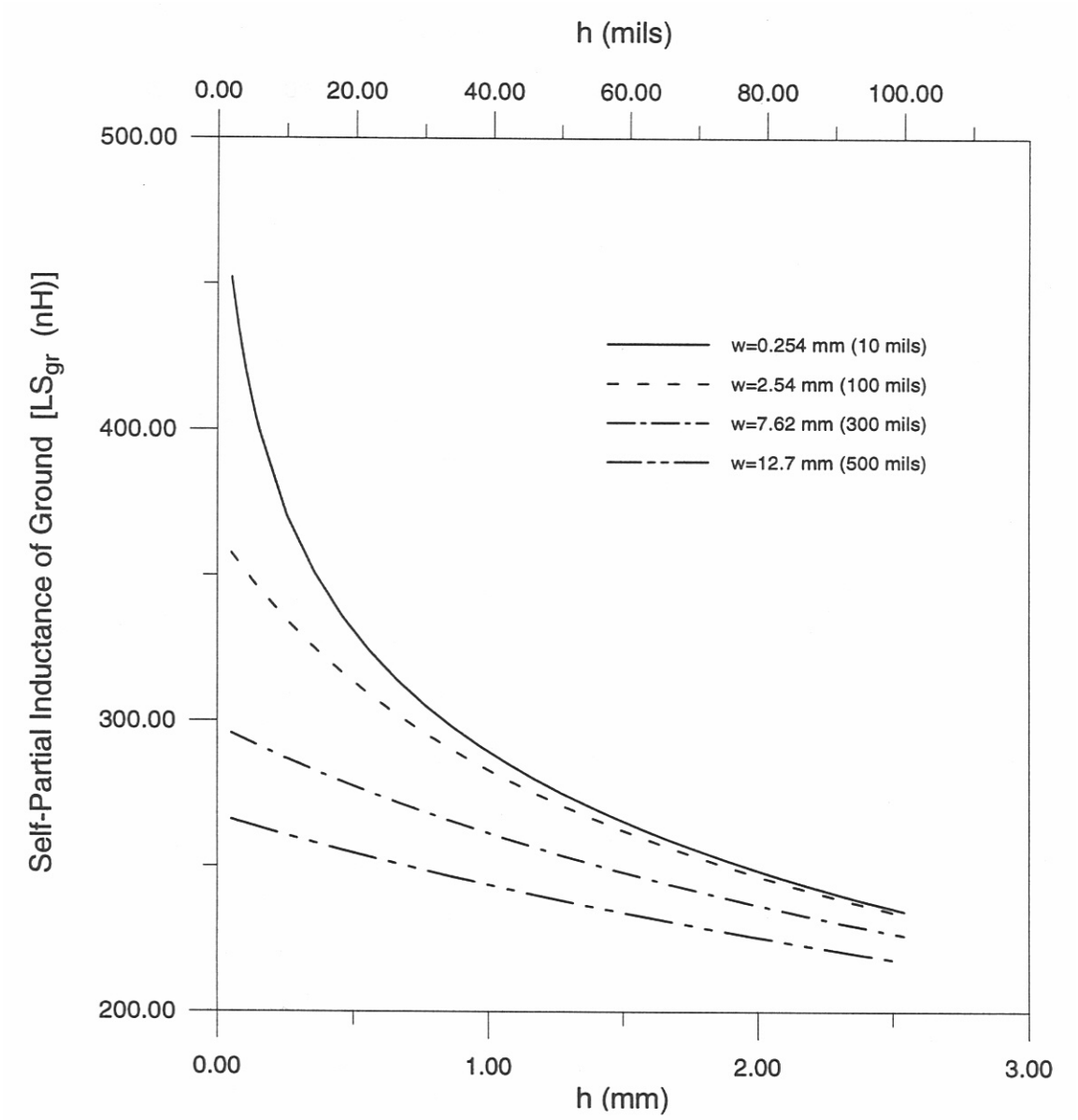

Figure 7. Self-partial inductance of the ground plane as a function of the trace width *w* and the height over the ground *h* for trace length *l* of 30.48 cm (12 in).

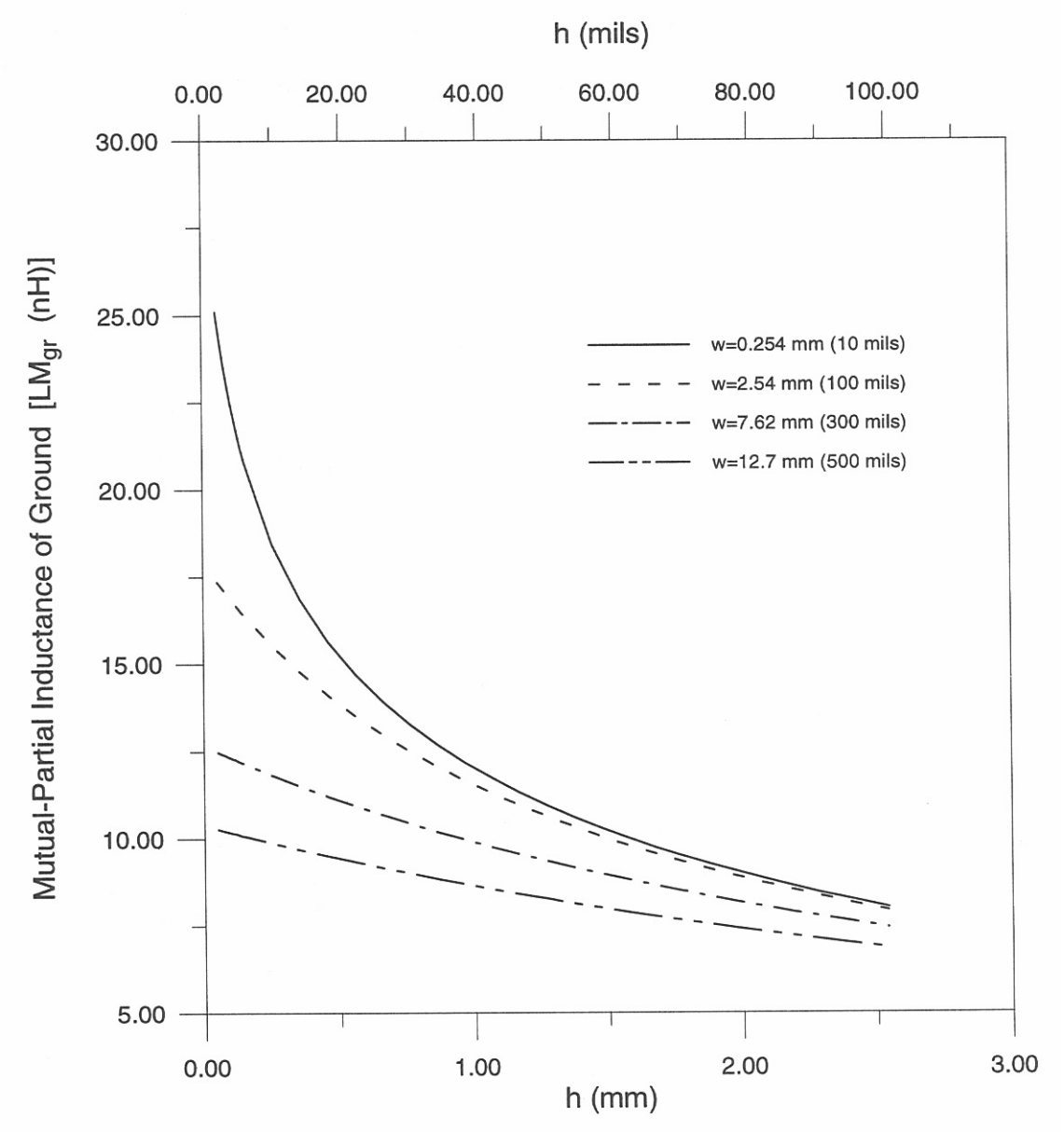

Figure 8. Mutual-partial inductance of the ground plane as a function of the trace width *w* and the height over the ground *h* for trace length *l* of 2.54 cm (1 in).

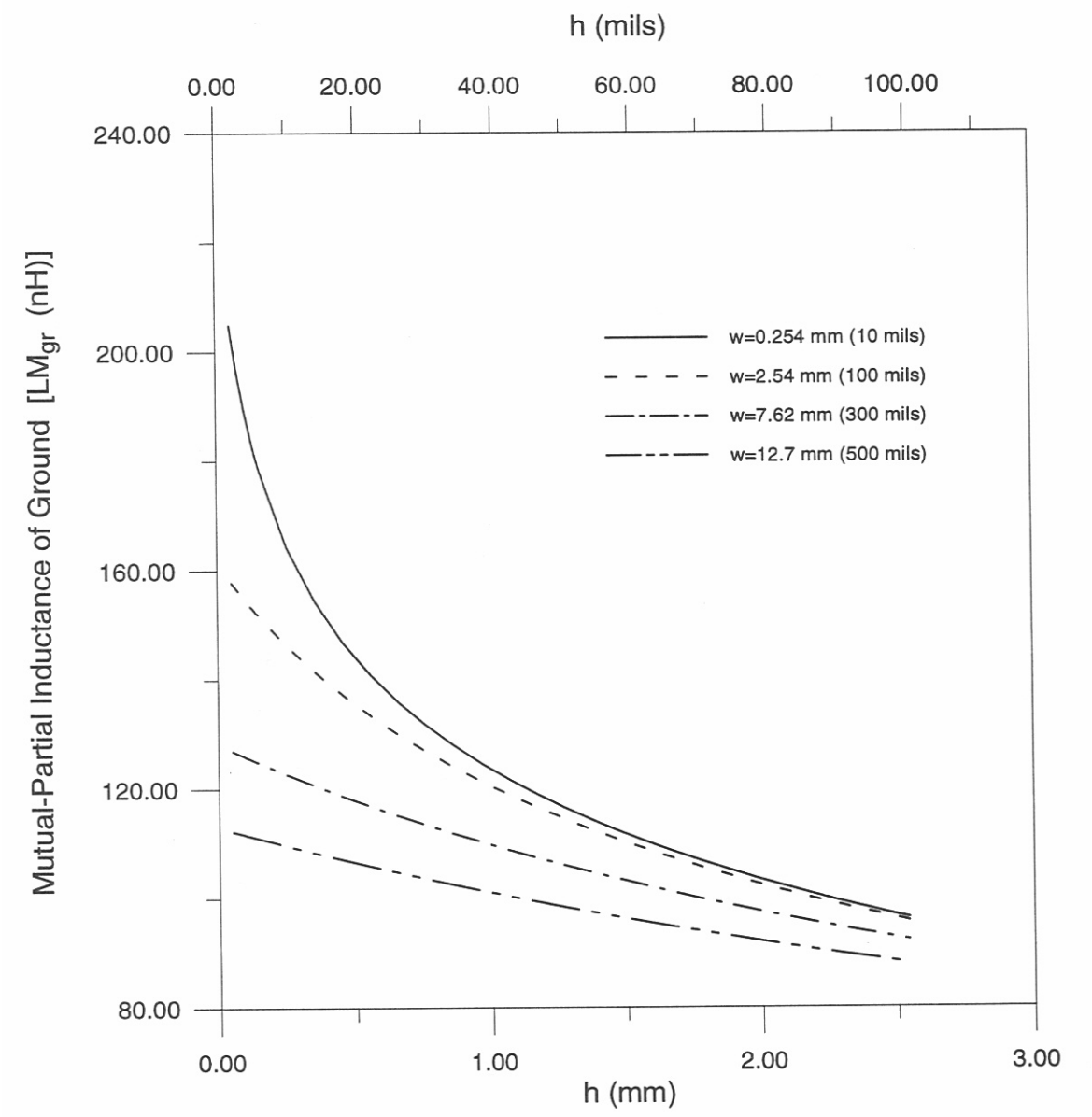

Figure 9. Mutual-partial inductance of the ground plane as a function of the trace width *w* and the height over the ground *h* for trace length *l* of 15.24 cm (6 in).

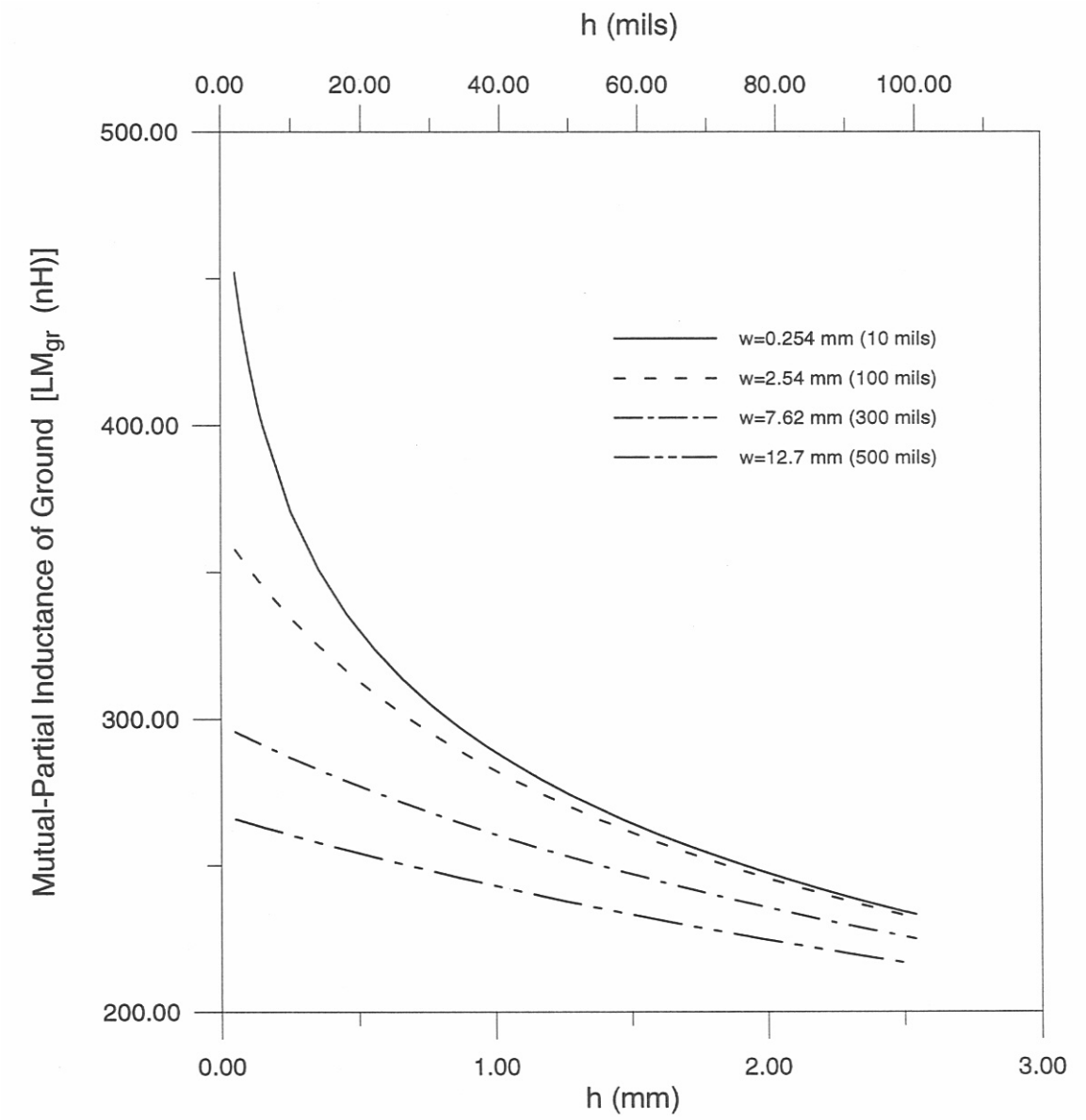

Figure 10. Mutual-partial inductance of the ground plane as a function of the trace width *w* and the height over the ground *h* for trace length *l* of 30.48 cm (12 in).

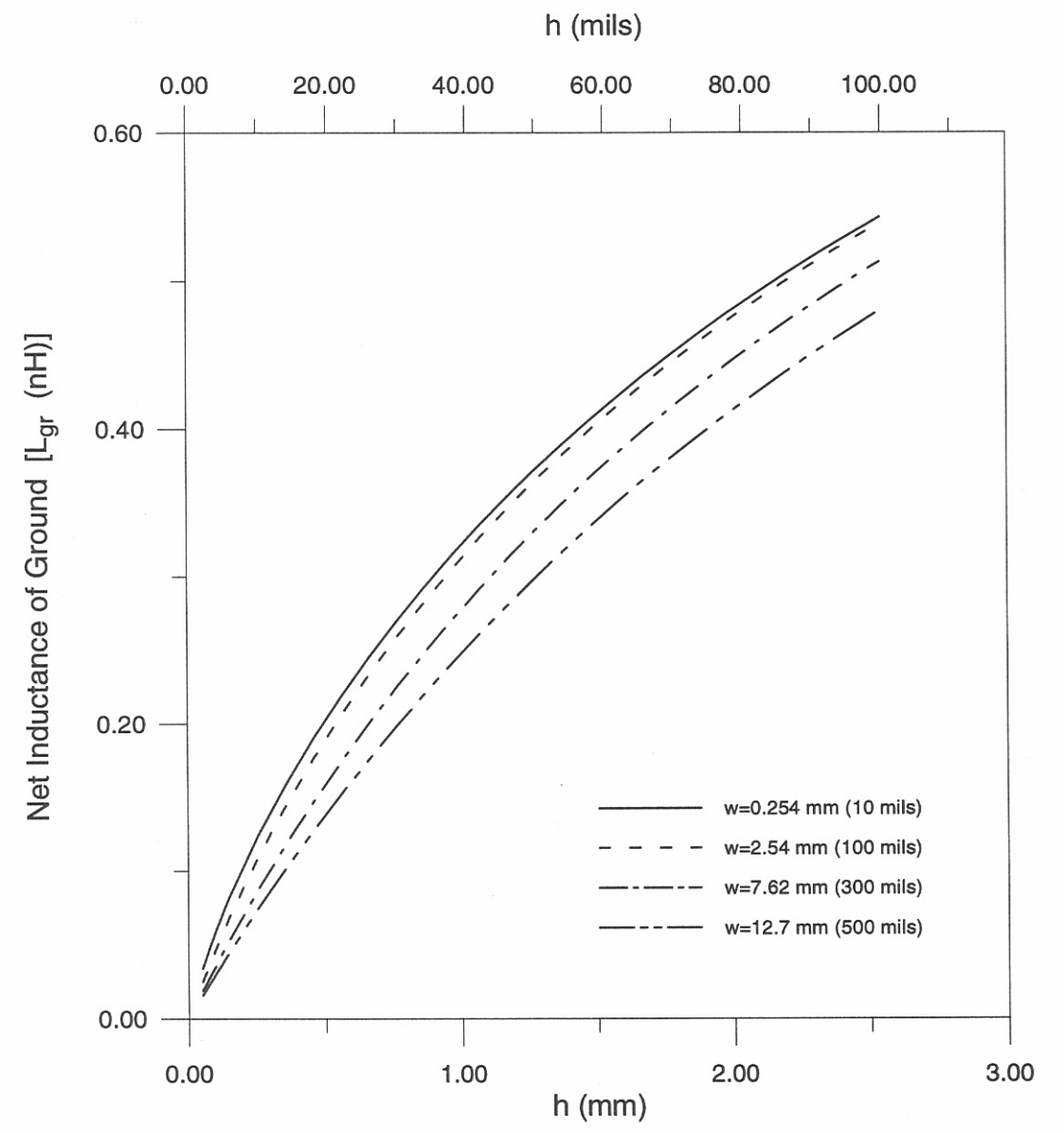

Figure 11. Net inductance of the ground plane as a function of the trace width *w* and the height over the ground *h* for trace length *l* of 2.54 cm (1 in).

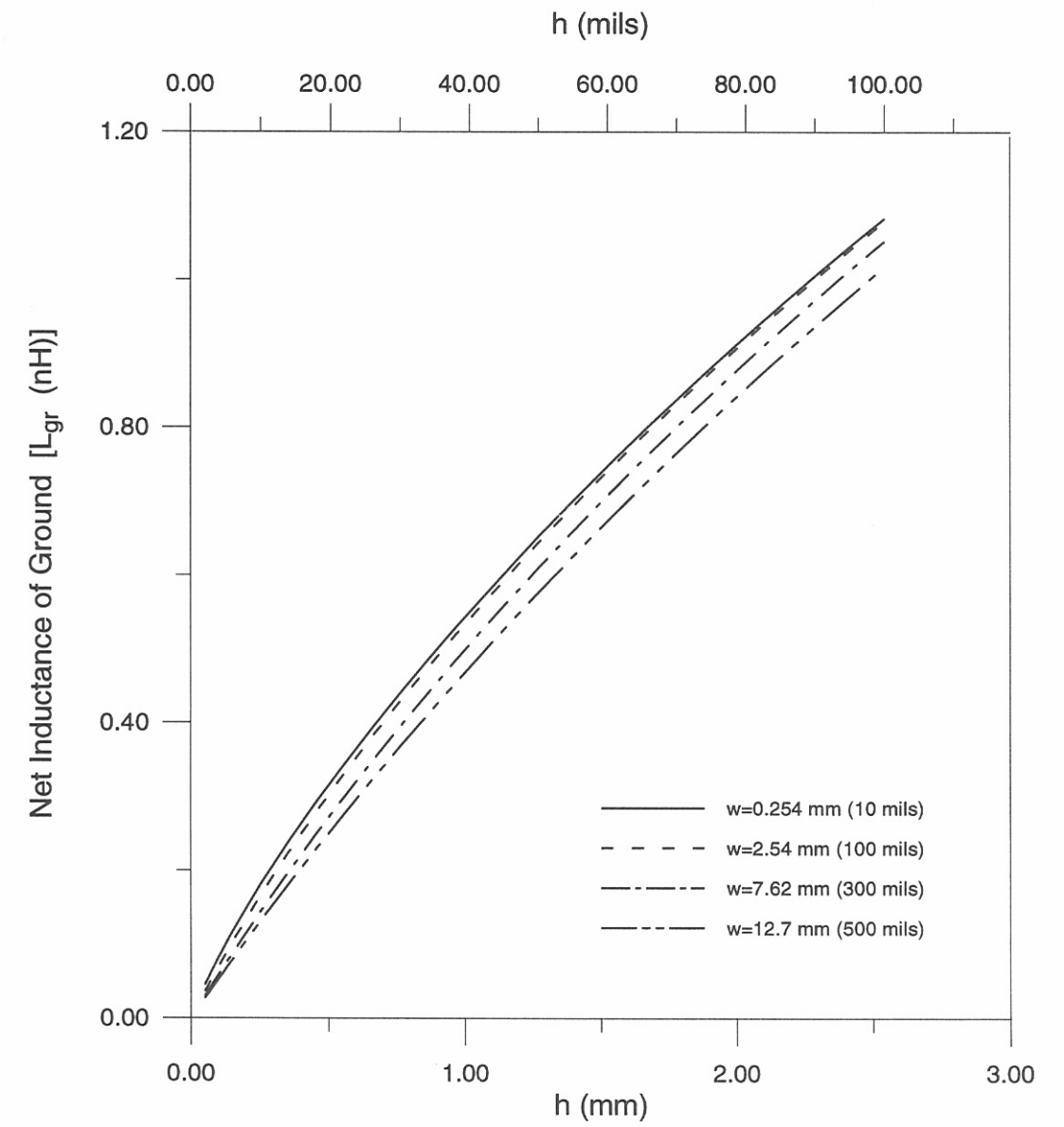

Figure 12. Net inductance of the ground plane as a function of the trace width *w* and the height over the ground *h* for trace length *l* of 15.24 cm (6 in).

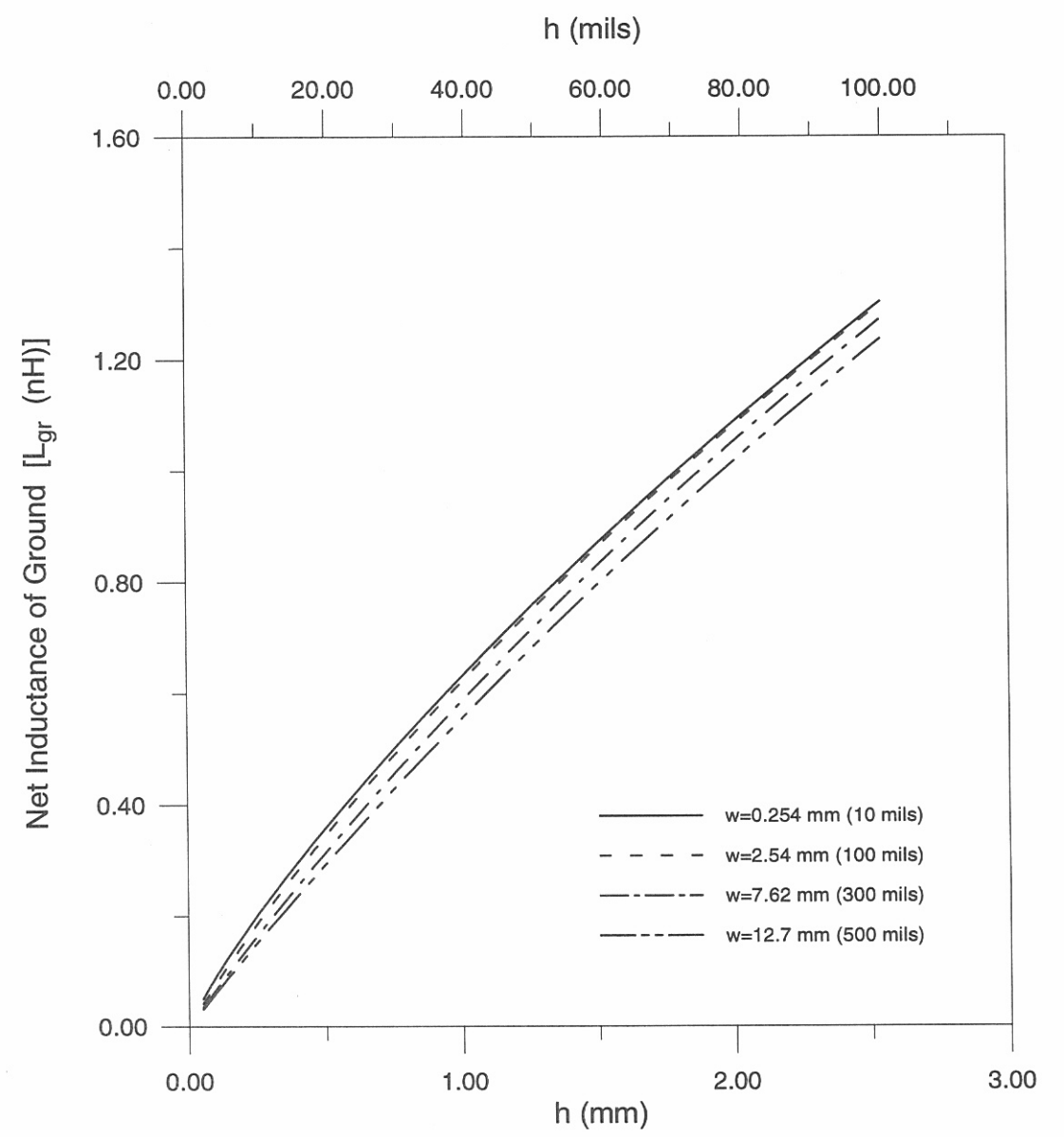

Figure 13. Net inductance of the ground plane as a function of the trace width *w* and the height over the ground *h* for trace length *l* of 30.48 cm (12 in).

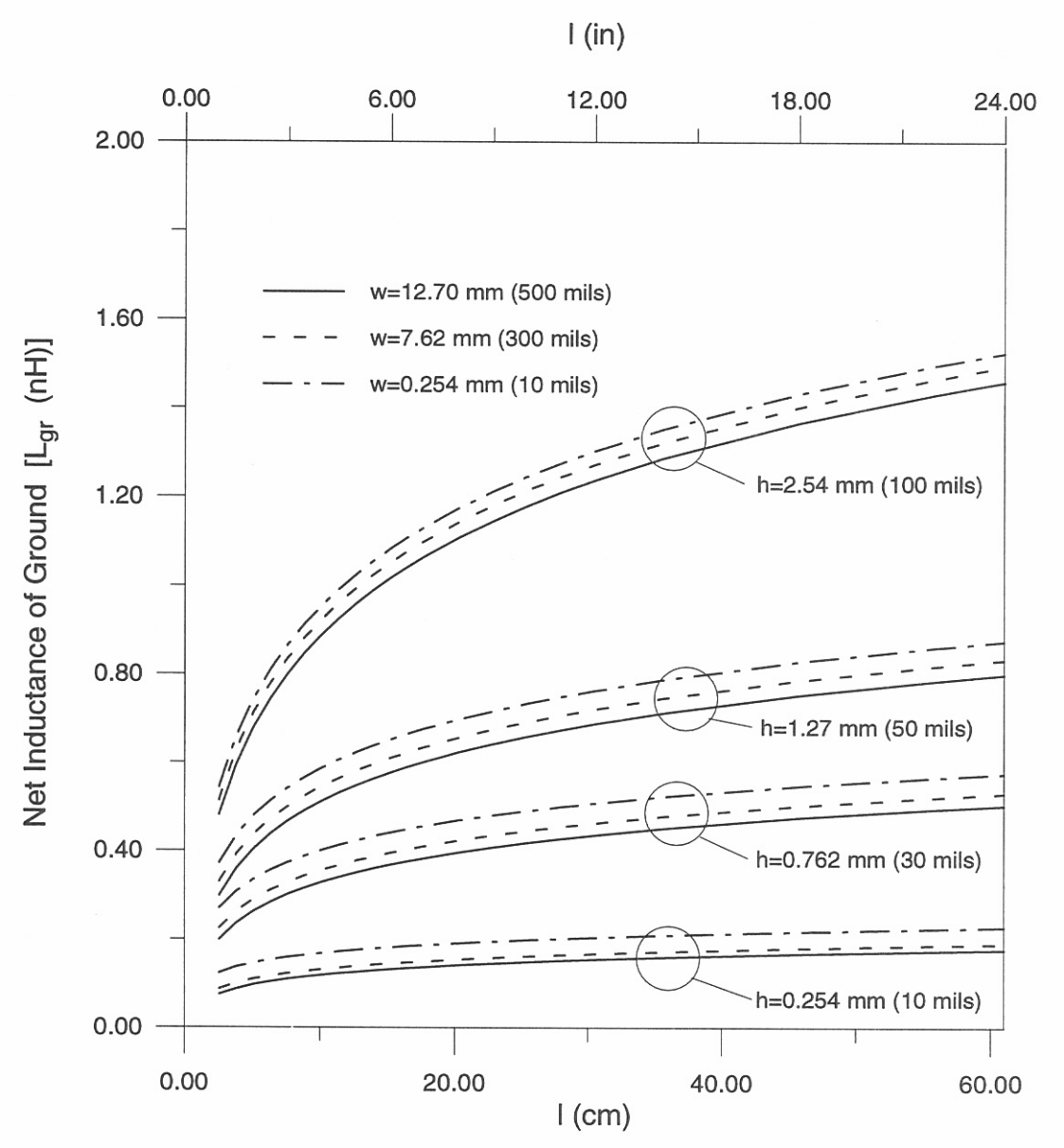

Figure 14. Net inductance of the ground plane as a function of the trace height *h,* the trace width *w,* and the trace length *l.*

While this reduction in the voltage-drop (net inductance) we calculated is for an idealized perfectly conducting infinitely large ground plane with balanced currents flowing on the ground and trace, it illustrates how the voltage-drop of the actual problem (finite ground plane with unbalanced currents on the ground and trace) varies as a function of the height h and width w of the trace. Therefore, the reduction in the voltage-drop on the ground plane (due to the reduction of the trace height *h),* decreases the source driving the common-mode emissions, and more importantly results in a dramatic reduction of the common-mode emissions of the board.

The substantial reduction of the net inductance of the ground plane L_{gr} for small values of h can be explained by referring to equations (44) and (49). These two equations represent the self- and mutual-partial inductance of the ground, and as h gets small these two expressions approach one another for two reasons. First, one of the differences in these integrals is that the outer integral for the mutual-partial inductance is evaluated to $\pm w/2$ with $J = I/w$. From equation (16) and [24] it can be shown that as the height of the trace becomes small, the current of the ground plane is concentrated under the trace and very little current spreads out past the trace edges. For very small h values, the current distribution on the ground plane can be approximated as a constant (e.g., $J_{gr} \approx I/w$). Therefore, for very small h values, the limit to infinity on the integral in equations (44) and (49) can be evaluated to $\pm w/2$. If this approximation is made for small h values, then the only difference in the self- and mutual-partial inductance is the kernel *(*K_1*,* K_2*,* and K_m*)*. Based on equations (42), (43), and (50), it is seen that for very small h values,

$$\lim_{h\to 0}\left[K_m - \left(K_1 + K_2\right)\right] \Rightarrow 0 . \tag{63}$$

Therefore, for small h values, the net inductance of the ground plane L_{gr} approaches zero:

$$\lim_{h\to 0} L_{gr} = LS_{gr} - LM_{gr} \Rightarrow 0 . \tag{64}$$

That is to say that for small h values, the mutual-partial inductance LM_{gr} approaches the self-partial inductance LS_{gr}.

The results for the self-partial inductance of the trace LS_{tr} are shown in Figure 15. Note that the self-partial inductance of the trace is not a function of h (the trace height). This is because we have assumed that the current density on the trace is not a function of h. The net inductance of the trace L_{tr} can be obtained from equation (52). Figures 16-18 show results of the net inductance of the trace L_{tr} for various geometries. Note, that for the same geometries, the net inductance of the trace L_{tr} is significantly larger than that of the net inductance of the ground L_{gr}.

6. VALIDATION OF RESULTS

For validation, we compared the ground plane inductance obtained with the techniques presented here to measured data. There is limited measured data of the ground plane net

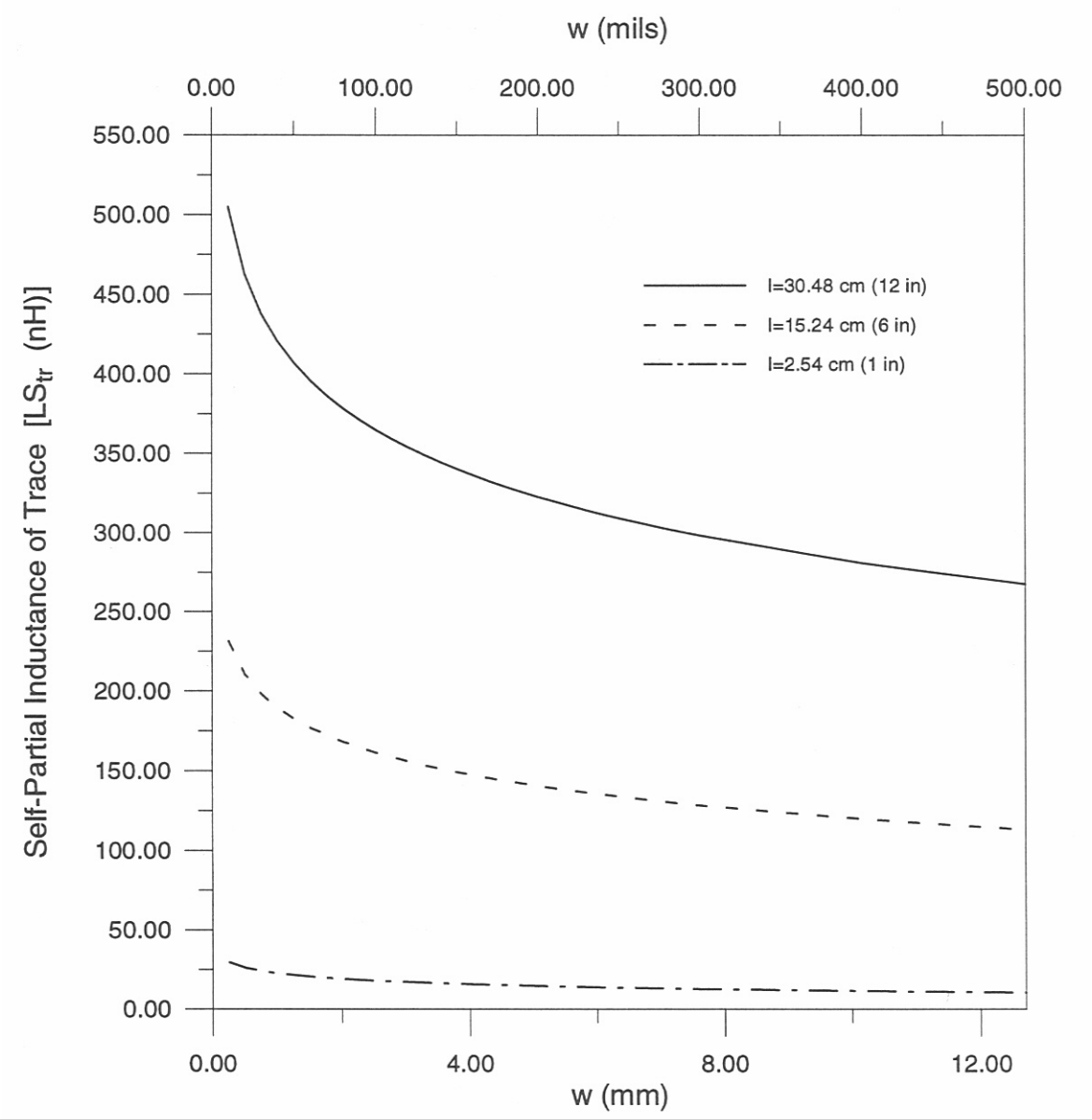

Figure 15. Self-partial inductance of the trace as a function of the trace width *w* for trace length *l* of 2.54 cm (1 in), 15.24 cm (6 in), and 30.48 cm (12 in), respectively.

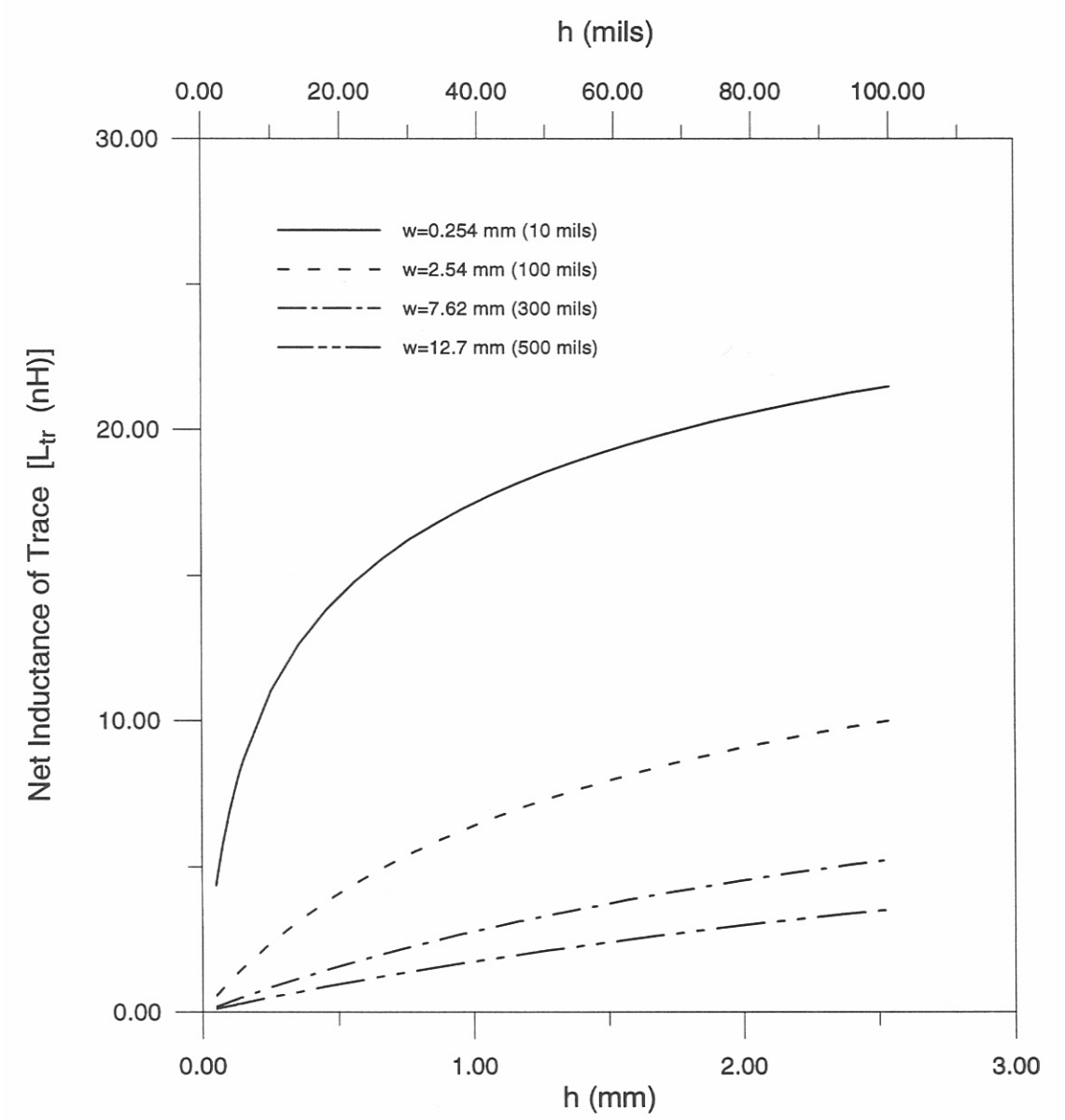

Figure 16. Net inductance of the trace as a function of the trace width *w* and the height over the ground *h* for trace length *l* of 2.54 cm (1 in).

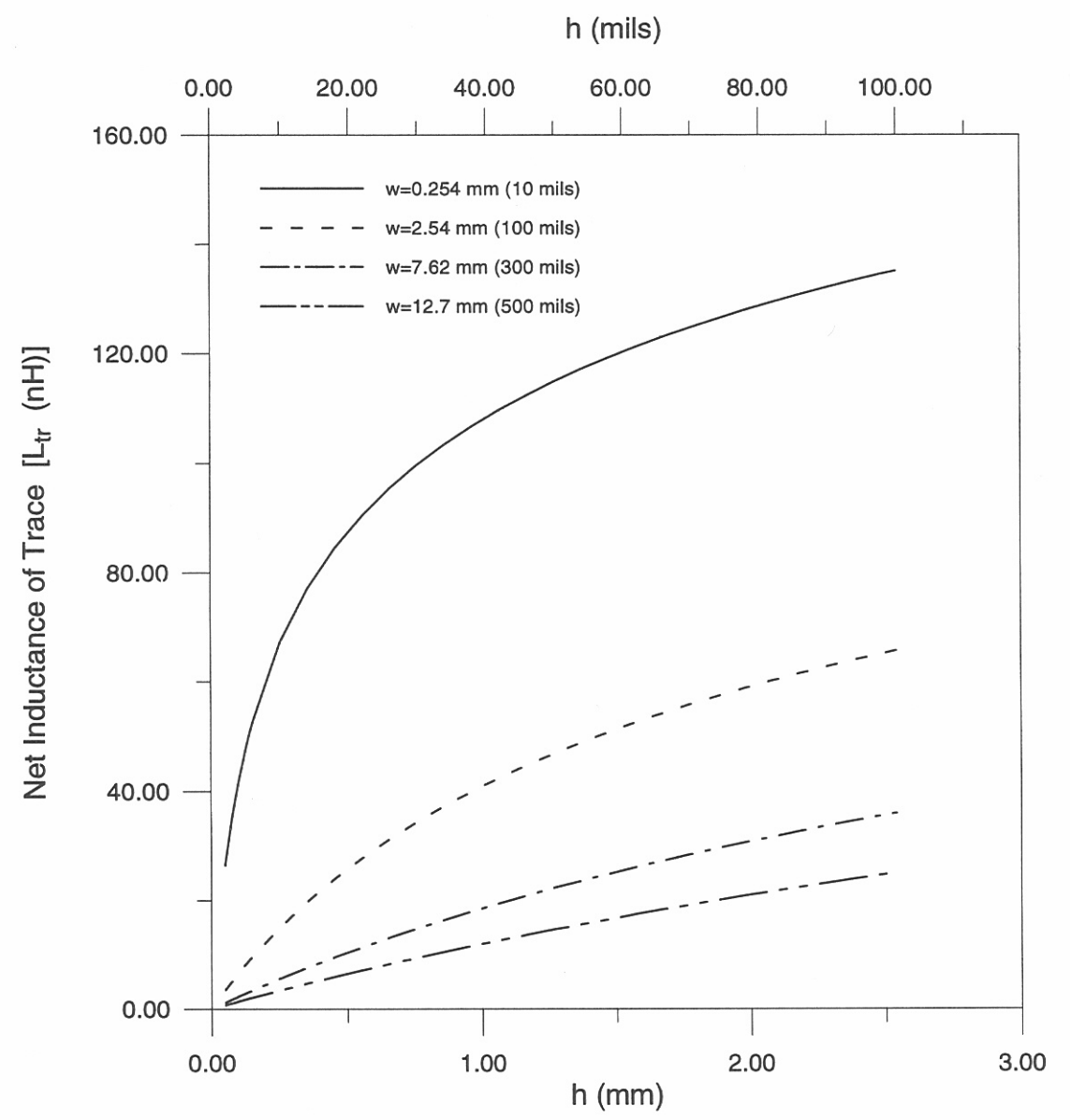

Figure 17. Net inductance of the trace as a function of the trace width *w* and the height over the ground *h* for trace length *l* of 15.24 cm (6 in).

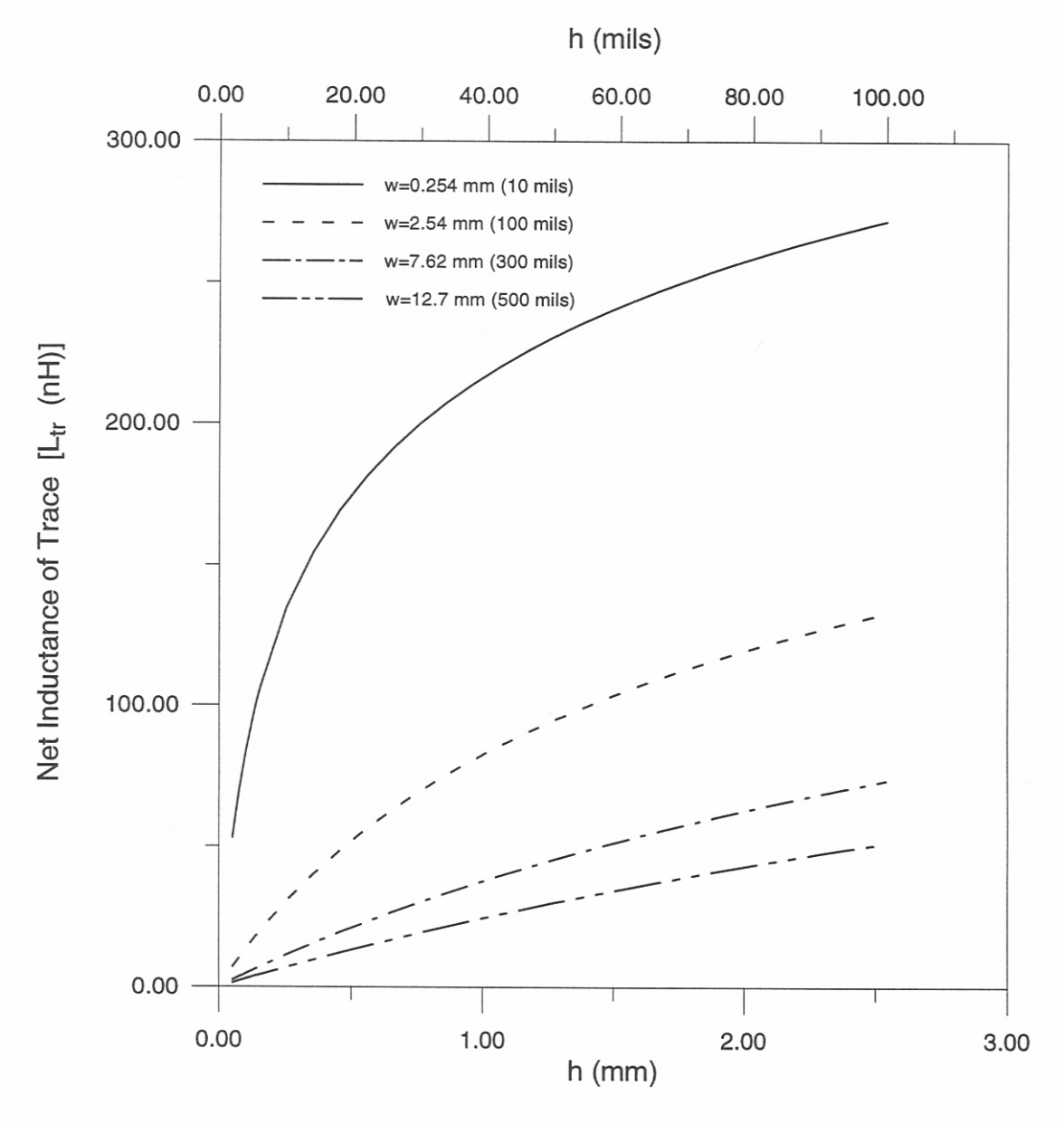

Figure 18. Net inductance of the trace as a function of the trace width *w* and the height over the ground *h* for trace length *l* of 30.48 cm (12 in).

inductance. Basically, the only measured data are that of Ott [33] and Leferink [34]. In [33], Ott measured the ground plane inductance for a trace of w = 2.54 mm (100 mils), h = 1.575 mm (62 mils), and l = 15.24 cm (6 in). In these measurements, Ott determined the ground plane inductance for a 2.54-cm (1 in) segment at the center of the 15.24-cm (6 in) line. By performing the measurements at the center of the line, the end effects can be minimized. The current at the ends of the line is forced to constrict (due to vias), which causes the inductance at the ends to increase. (The increase of inductance due to current constriction at the ends is discussed in the next section.) For the above geometry, Ott measured a net inductance of the ground plane L_{gr} to be approximately 0.5 nH. Using our model, we calculated the ground plane net inductance L_{gr} for this same geometry to be 0.42 nH. Ott indicates that his measurement error is about ±20%. Based on this margin of error, our results correlate well with Ott's measurements.

Leferink [34] measured the ground plane inductance for a length of l = 0.3 m (11.81 in), h = 1.6 (63 mils), and w = 2.2 mm (87 mils). Leferink's so-called immunity method determined the ground plane inductance to be 0.96 nH. We calculated the ground plane net inductance L_{gr} for this geometry to be 0.91 nH. Once again, good correlation between the theory and measurement was demonstrated.

Notice that the geometry that Leferink investigated has essentially the same height and width of that investigated by Ott. The main difference is that Leferink measured the net inductance for a length of l = 0.3 m, which is about a factor of 10 larger than in Ott's example. The good correlation to both Ott's and Leferink's measurements illustrates that our results properly account for the behavior of the net inductance as a function of length.

Comparison of a third experiment by Dockey and German [17] allowed us to investigate how well our model can predict differential ground plane inductance. Dockey and German [17] measured the difference between the emissions of two traces with different heights. In the first trace, h = 1.575 mm (62 mils) and w = 2.286 mm (90 mils); and in the second trace, h = 0.1778 mm (7 mils) and w = 0.381 mm (15 mils). The width of the traces was changed to ensure that the impedance of both the traces was the same. Dockey and German measured on average a 12- to 13-dB reduction in emissions for the smaller h value. The reduction in the height corresponded to a small cross-sectional area of the current loop (the trace and ground plane loop). The new cross-sectional area was only 11% of the original area. Since the emissions due to the differential-mode currents are proportional to the cross-sectional area of the loop, these measured reductions in emissions cannot be accounted for by the differential-mode current (the loop antenna), and are associated with common-mode emissions (or a change in the ground plane net inductance L_{gr}).

For a trace height of 1.575 mm (62 mils) and a width of 2.286 mm (90 mils) our model predicted a ground plane inductance of 0.42 nH; and for a trace height of h = 0.1778 mm (7 mils) and a width of 0.381 mm (15 mils), our model predicted a ground plane inductance of 0.09 nH. If it is assumed that the voltage drop across the ground plane is the

dominant emission source, then the ratio of these two calculated ground inductances would indicate about a 13-dB reduction in emissions. Our model correlates well with the measured differential ground plane inductance of Dockey and German.

For a final validation of the results presented here, we calculated the inductance of the microstrip line with net and partial inductance. An expression for the inductance of a microstrip line with an accuracy of 2% was derived by Wheeler [35] and is given by:

$$L_{TEM} = l\frac{\mu_0}{4\pi}\ln\left\{1+\frac{32h^2}{w^2}\left[1+\sqrt{1+\left(\frac{\pi w^2}{8h^2}\right)^2}\right]\right\}. \tag{65}$$

The inductance of the microstrip line can also be approximated with net inductance by summing the net inductance of the ground L_{gr} and trace L_{tr}:

$$L \approx L_{gr} + L_{tr}. \tag{66}$$

Figure 19 shows a comparison of the inductance of a microstrip line obtained from these two expressions for l = 30.48 cm (12 in) and various values of h and w. This comparison shows that the deviation of the inductance of the microstrip line obtained by equation (66) from that of equation (65) ranges from 2-5%. Secondly, notice that the net inductance of the trace L_{tr} dominates the net inductance of the ground plane L_{gr} and is the dominant term in the microstrip inductance given in equation (66).

7. EXCESS INDUCTANCE DUE TO CURRENT CONSTRICTION

A discussion is in order concerning the effects of current constriction on the ground plane at the ends of a trace. In this study, we used the ground plane current distribution given in [24] (see equation (16)) which was derived assuming that the length of the microstrip was infinite. That is, effects of the ends were not taken into account.

On the ground plane, the current behaves as follows: in the region away from the ends (Region B in Figure 20), the current spreads out from under the trace and is governed by equation (16). In the regions close to the ends (Regions A and C in Figure 20) the current on the ground plane is forced back under the trace. This occurs because the current on the ground is forced into the via that connects the trace to the ground. Figure 20 shows how the current flows in these three regions.

The constriction of the ground plane current at the ends of the trace causes the inductance of the line to increase. The calculations in the previous section do not account for the added inductance due to current constriction. An exact calculation of this added inductance requires solving a three-dimensional electromagnetic problem. Kok and De Zutter [36] and Swanson [37] analyzed a similar problem found in MIMIC circuits and indicate that this type of calculation can be very involved. A detailed calculation of this added inductance due to the current constriction at the end of the trace will be a topic of future investigation.

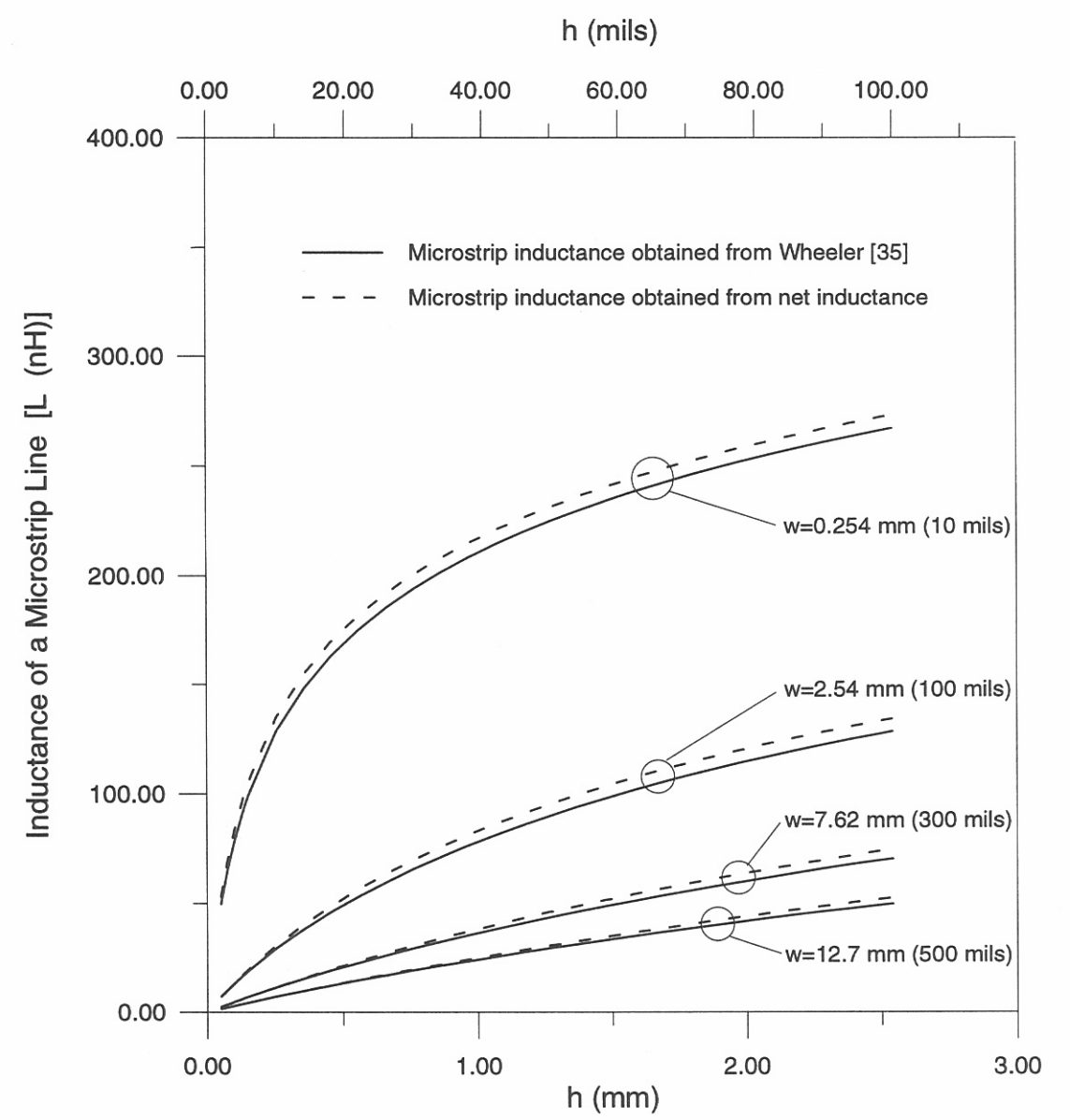

Figure 19. Inductance of a microstrip line as a function of the trace width *w* and the height over the ground *h* for trace length *l* of 30.48 cm (12 in).

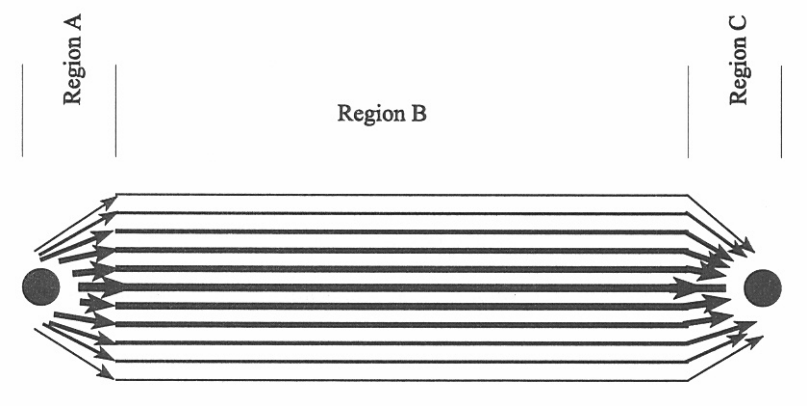

Figure 20. Illustration of how the current of the ground plane is forced to concentrate at the end due to the via.

In this section, a qualitative discussion of the added inductance is given for the case when $h << w$. For convenience, it is assumed that the via from the trace to the ground plane is simply an extension of the trace itself (Figure 21). The current on the ground will then be forced inward at the ends. At the end of the trace, the current on the ground plane will be distributed within the $\pm w/2$ region. We showed [24] that the amount the current on the ground plane spreads out from the edge of the trace is decreased by making h small. If h is small, the current is constricted under the trace and very little current spreads out from the $\pm w/2$ region. For small h values, the current distribution close to the end (or via) is the same as the current distribution far from the end. The distribution of the current on the ground plane is uniform over the whole length of line. Therefore, for small h values, the added inductance associated with current constriction at the ends is negligible.

Finally, it should be noted that besides the added inductance caused by the current constriction, there is an additional inductance at the end of the trace that is associated with the connection of components and devices to the trace. This inductance may also need to be considered.

8. CONCLUSION

In this report, a model for calculating the net inductance of a ground plane and the trace was presented. The calculation of these inductances is based on a previously derived expression for the current distribution on the ground plane. Due to the complicated integrals in the formulas given here, it is not possible to develop closed form expressions for these net inductances. Given, however, are curves for the calculated net inductances (as well as the self- and mutual-partial inductance) of the ground plane and trace for various trace geometries of practical interest. These curves can be used in designing printed circuit boards. Results

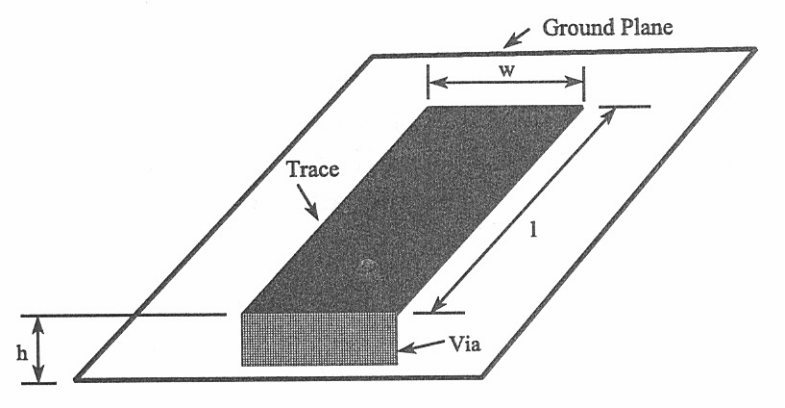

Figure 21. Illustration of a via of width *w*.

from this model were compared to three different sets of experimental data and excellent correlation was demonstrated.

It was shown that the net inductance of the ground plane is affected more by changes in the height *h* of the trace than by changes in the width *w* of the trace. Moderate changes in the height *h* of the trace can drastically decrease the net inductance of the ground plane, and more importantly can dramatically reduce the voltage-drop across the ground plane, and in turn lower the printed circuit board emissions. In summary, emissions from the printed circuit board trace can be reduced by making *h* smaller because of the following two reasons. First, the added end inductance due to current constriction is negligible, and second, the smaller the value of *h,* the smaller the net inductance of the ground plane.

9. ACKNOWLEDGMENTS

The authors would like to thank R.F. German of German Training and Consulting, LLC for his helpful discussions, encouragement, and technical assistance.

10. REFERENCES

[1] C.R. Paul, *Introduction to Electromagnetic Compatibility,* New York: John Wiley & Sons, Inc., 1992, chapter 2.

[2] Ibid., chapter 13.

[3] D.M. Hockanson, J.L. Drewniak, T.H. Hubing, T.P. Van Doren, F. Sha, and M.J. Wilhelm, "Investigation of fundamental EMI source mechanisms driving common-mode radiation from printed circuit boards with attached cables," *IEEE Trans. Electromag. Compat.,* vol. 38, no. 4, pp. 557-566, 1996.

[4] op.cit. Paul, chapter 8.

[5] H.W. Ott, *Noise Reduction Techniques in Electronic Systems (second edition),* New York: John Wiley Interscience, 1988, chapter 11.

[6] J.R. Bergervoet, "EMC measurements and models connecting the system level with the module level," *Philips J. Res.,* vol. 48, no. 1-2, pp. 63-81, 1994.

[7] C.R. Paul, "A comparison of the contributions of common-mode currents and differential-mode currents in radiated emissions," *IEEE Trans. Electromag. Compat.,* vol. 31, no. 2, pp. 189-193, 1989.

[8] C.R. Paul and D.R. Bush, "Radiated emissions from common-mode currents," in *Proc. 1987 IEEE Internat. Symp. Electromag. Compat.,* Atlanta, Ga., 1987, pp. 197-203.

[9] R.F. German, H.W. Ott, and C.R. Paul, "Effect of an image plane on printed circuit board radiation," in *Proc. 1990 IEEE Internat. Symp. Electromag. Compat.,* Washingtion, 1990, pp. 284-291.

[10] J.T. Fessler, K.W. Whites, and C.R. Paul, "Effect of image plane dimensions on radiated emissions," in *Proc. 1992 IEEE Internat. Symp. Electromag. Compat.,* Anaheim, CA, 1992, pp. 106-111.

[11] T.A. Jerse, C.R. Paul, and K.W. Whites, "The effect of finite image plane width on the radiation from an electric line source," in *Proc. 10th Internat. Zurich Symp. and Technical Exhibition Electromag. Compat.,* Zurich, 1993, pp. 201-206.

[12] T.S. Smith and C.R. Paul, "Effect of grid spacing on the inductance of ground grids," in *Proc. 1991 IEEE Internat. Symp. Electromag. Compat.,* Cherry Hill, New Jerry, 1991, pp. 72-77.

[13] op.cit. Ott, chapter 10.

[14] R.F. German, "Use of a ground grid to reduce printed circuit board radiation," in *Proc. 6th Symp. and Technical Exhibition on Electromag. Compat.,* Zurich, 1985, pp. 133-138.

[15] H.W. Ott, "Digital circuit grounding and interconnection," in *Proc. 1981 IEEE Internat. Symp. Electromag. Compat.,* Boulder, CO, 1981, pp. 292-297.

[16] R.W. Dockey, "Asymmetrical mode radiation from multi-layer printed circuit boards," in *Proc. 1992 EMC/ESD Internat.,* Denver, CO, 1992, pp. 247-251.

[17] R.W. Dockey and R.F. German, "New techniques for reducing printed circuit board common-mode radiation," in *Proc. 1993 IEEE Internat. Symp. Electromag. Compat.,* Dallas, TX., 1993, pp. 334-338.

[18] Title 47, Code of Federal Regulations, Part 15, Subpart B**,** section 15.109, October 1, 1995.

[19] A.E. Ruehli, "Inductance calculations in a complex integrated circuit environment," *IBM J. Res. Develop,* vol. 16, no. 5, pp. 470-481, 1979.

[20] C.R.Paul, "Modeling electromagnetic interference properties of printed circuit boards," *IBM J. Res. Develop.,* vol. 33, no. 1, pp. 33-50, 1989.

[21] C. Hoer and C. Love, "Exact inductance equation for rectangular conductors with applications to more complicated geometries," *J. Res. Nat. Bureau of Standards-C. Eng. Instrum.,* vol. 69C, no. 2, pp. 127-137, 1965.

[22] F.W. Grover, *Inductance Calculations: Working Formulas and Tables,* New York: Dover Publications, Inc. (by the Instrument Society of America), 1973.

[23] F.B.J. Leferink and M.J.C.M. van Doorn, "Inductance of printed circuit board ground planes," in *Proc. 1993 IEEE Internat. Symp. Electromag. Compat.,* Dallas, TX., 1993, pp. 327-329.

[24] C.L. Holloway and E.F. Kuester, "Closed-form expressions for the current density on the ground plane of a microstrip line, with application to ground plane loss," *IEEE Trans. Microwave Theory and Tech.,* vol. 43, no. 5, pp. 1204-1207, 1995.

[25] C.L. Holloway, "Edge and surface shape effects on conductor loss associated with planar circuits," MIMICAD Technical Report No. 12, Electromagnetic Laboratory, Department of Electrical and Computer Engineering, University of Colorado at Boulder, Appendix G, 1992.

[26] M. Wien, "Ueber die Berechnung und messung kleiner selbstpotentiale," *Annalen der Physik und Chemie,* band 53, heft 5, pp. 928-947, 1894.

[27] E.B. Rosa, "The self and mutual inductance of linear conductors," *Bulletin of the Bureau of Standards,* vol. 4, no. 2, pp. 301-344, 1907.

[28] E.B. Rosa and F.W. Grover, "Formulas and tables for the calculation of mutual and self-inductance," *Bulletin of the Bureau of Standards,* vol. 8, no. 1, pp. 1-230, 1912.

[29] C.T.A. Johnk, *Engineering Electromagnetic Fields and Waves,* New York: John Wiley & Sons, 1975, chapter 5.

[30] C.L. Holloway and E.F. Kuester, "Edge shape effects and quasi-closed form expressions for the conductor loss of microstrip lines," *Radio Science,* vol. 29, no. 3, pp. 539-559, 1994.

[31] C.G. Harris and W.A.B. Evans, "Extension of numerical quadrature formulae to singular behaviors over finite intervals," *Intern. J. Computer Math., Section B,* vol. 6, pp. 219-227, 1977.

[32] W.H. Press, B.P. Flannery, S.A. Teukolsky, and W.T. Vetterling, *Numerical Recipes: The art of Scientific Computing,* New York: Cambridge University Press, 1986, Chapter 4, pp. 120-126.

[33] H.W. Ott, "Empirical determination of ground-plane inductance," *Regional Symp. on EMC, IEEE EMC Society, Rocky Mountain Chapter,* Boulder, CO, 1994.

[34] F.B.J. Leferink, "Inductance calculations; experimental investigations," in *Proc. 1996 IEEE Internat. Symp. Electromag. Compat.,* Santa Clara, CA., 1996, pp. 235-240.

[35] H.A. Wheeler, "Transmission-line properties of a strip on a dielectric sheet on a plane," *IEEE Trans. Microwave Theory and Tech.,* vol. 25, no. 8, pp. 631-647, 1977.

[36] P.A. Kok and D. De Zutter, "Scalar magnetostatic potential approach to the prediction of the excess inductance of grounded via's and via's through a hole in a ground plane," *IEEE Trans. Microwave Theory and Tech.,* vol. 42, no. 7, pp. 1229-1237, 1994.

[37] D.G. Swanson, "Grounding microstrip lines with via holes," *IEEE Trans. Microwave Theory and Tech.,* vol. 40, no. 8, pp. 1719-1721, 1992.

APPENDIX: GENERAL PURPOSE 10-POINT QUADRATURE WEIGHTS

The weights A_i and abscissae x_i used in this report are from Harris and Evans [1] and are listed in the Table below. These are the values used for the integrals with both the singular and nonsingular kernels.

General Purpose 10-point Quadrature Weights A_i and Abscissae x_i Values

x_i	A_i
0.2295037173828339858 3	0.4501100825389664199 7
0.6364758400917634814 5	0.3483026851774169233 9
0.9015072053318363871 8	0.1744679766182790900 7
0.9928383122352035294 46	0.0269629977216037852 57
0.9999843442623408409287	0.0001562579437337813003

REFERENCE

[1] C.G. Harris and W.A.B. Evans, "Extension of numerical quadrature formulae to singular behaviors over finite intervals," *Intern. J. Computer Math., Section B,* vol. 6, pp. 219-227, 1977.

FORM **NTIA-29**
(4-80)

U.S. DEPARTMENT OF COMMERCE
NAT'L. TELECOMMUNICATIONS AND INFORMATION ADMINISTRATION

BIBLIOGRAPHIC DATA SHEET

	1. PUBLICATION NO.	2. Gov't Accession No.	3. Recipient's Accession No.
	98 - 344		

4. TITLE AND SUBTITLE

Analysis and Calculations of the Ground Plane Inductance Associated with a Printed Circuit Board

5. Publication Date
November 1997

6. Performing Organization Code
NTIA/ITS

7. AUTHOR(S)
Christopher L. Holloway, Edward F. Kuester

9. Project/Task/Work Unit No.
910 8105

8. PERFORMING ORGANIZATION NAME AND ADDRESS

NTIA/ITS.S3
325 Broadway
Boulder, CO 80303-3328

10. Contract/Grant No.

11. Sponsoring Organization Name and Address

12. Type of Report and Period Covered

13.

14. SUPPLEMENTARY NOTES

15. ABSTRACT *(A 200-word or less factual summary of most significant information. If document includes a significant bibliography or literature survey, mention it here.)*

A knowledge of the partial inductance of the ground plane can aid in the analysis and investigation of printed circuit board emissions. In this paper we present a method to determine the partial inductance of the ground plane associated with a microstrip line. This method is based on a previously derived expression for the current density on the ground plane. We show calculations for the partial inductance of the ground plane for various trace geometries of practical interest. We also illustrate how the classical transmission line inductance of a microstrip line can be obtained from the concept of partial inductance. Comparisons to different experimental results are also given.

16. Key Words *(Alphabetical order, separated by semicolons)*

common-mode emissions; ground plane inductance; microstrip line inductance; partial inductance

17. AVAILABILITY STATEMENT

☒ UNLIMITED.

☐ FOR OFFICIAL DISTRIBUTION.

18. Security Class. *(This report)*	20. Number of pages
unclassified	45
19. Security Class. *(This page)*	**21. Price:**
unclassified	